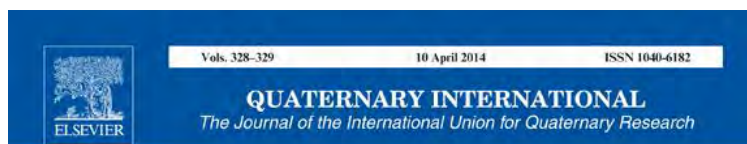


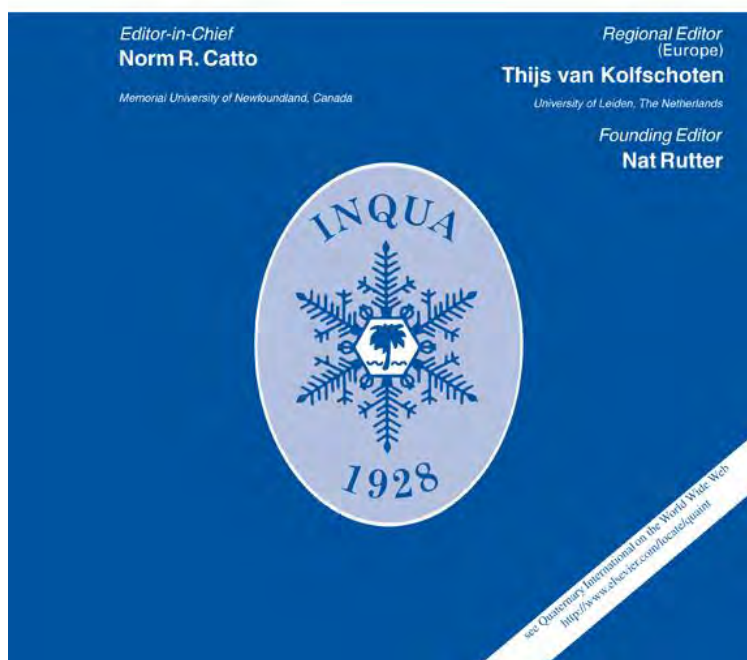
Provided for non-commercial research and education use.  
Not for reproduction, distribution or commercial use.



**SEQS 2012 SARDINIA: AT THE EDGE OF THE SEA**

*Guest Editors*

**VINCENZO PASCUCCI, MAURO COLTORTI AND PIERLUIGI PIERUCCINI**



This article appeared in a journal published by Elsevier. The attached copy is furnished to the author for internal non-commercial research and educational use, including for instruction at the author's institution and sharing with colleagues.

Other uses, including reproduction and distribution, or selling or licensing copies, or posting to personal, institutional or third party websites are prohibited.

In most cases authors are permitted to post their version of the article (e.g. in Word or Tex form) to their personal website or institutional repository. Authors requiring further information regarding Elsevier's archiving and manuscript policies are encouraged to visit:

<http://www.elsevier.com/copyright>



Contents lists available at ScienceDirect

## Quaternary International

journal homepage: [www.elsevier.com/locate/quaint](http://www.elsevier.com/locate/quaint)

## Dating and correlation of the Quaternary fluvial terraces in Syria, applied to tectonic deformation in the region



V.G. Trifonov<sup>a,\*</sup>, D.M. Bachmanov<sup>a</sup>, A.N. Simakova<sup>a</sup>, Ya.I. Trikhunkov<sup>a</sup>, O. Ali<sup>b</sup>,  
A.S. Tesakov<sup>a</sup>, E.V. Belyaeva<sup>c</sup>, V.P. Lyubin<sup>c</sup>, R.V. Veselovsky<sup>d</sup>, A.-M. Al-Kafri<sup>b</sup>

<sup>a</sup>Geological Institute of the Russian Academy of Sciences (RAS), 7 Pyzhevsky, Moscow 119017, Russia

<sup>b</sup>General Organization of Remote Sensing, P.O. Box 12586, Damascus, Syria

<sup>c</sup>Institute of the History of Material Culture of the RAS, 18 Dvortsovaya Naberezhnaya, S.-Petersburg, Russia

<sup>d</sup>Geological Faculty, Lomonosov State University, Moscow, Russia

### ARTICLE INFO

#### Article history:

Available online 21 November 2013

### ABSTRACT

New data on location, height, and composition of terraces of the El-Kabir and Orontes rivers in Syria are represented. By combined use of paleontological, archaeological, paleomagnetic, and radio-isotopic methods, ages of these river terraces are estimated and they are correlated with the Euphrates River terraces. The age of the terraces is defined more precisely by evidence of synchronism of the El-Kabir alluvial terraces and the marine terraces of the Mediterranean coast. The average rates of incision during different time intervals were estimated in the studied valleys and their segments using relative height of the terraces. This gives the possibility of approximately estimating a rate of the Quaternary uplift in different tectonic provinces of Syria as well as rates of vertical movements on the Lattaqieh (the El-Kabir valley), Hama (the Orontes valley), and Euphrates (the Euphrates valley) faults. The rates of incision were usually small in the earlier stages of the valley formation and increased later. The Middle and Late Pleistocene rates of the valley incision reach ~220–280 mm/ky in the El-Kabir valley (the Coastal Range-anticline), ~80–130 mm/ky in the Orontes valley and the Euphrates upstream of the Assad Reservoir (the mobile platformal Aleppo Block), and ~25–30 mm/ky in the Euphrates valley downstream of the Assad Reservoir (southwestern side of the Mesopotamian Foredeep).

© 2013 Elsevier Ltd and INQUA. All rights reserved.

### 1. Introduction

The aim of the paper is to estimate the Quaternary relative vertical movements in different tectonic provinces of Syria by using characteristics of the Quaternary terraces of large rivers. Because this estimation rests on the correctness of chronological correlation of the river terraces, the main attention is given to defining the ages of the terraces by a combination of dating methods, including geological and geomorphological studies, radio-isotopic dating, archaeology, paleontology (molluscs, mammals, and palynology), and magneto-stratigraphy. We studied three large rivers of the region: El-Kabir, Orontes, and Euphrates.

In this paper, we use the new stratigraphic division of the Pliocene and Quaternary, confirmed in the 33rd IGC ([www.stratigraphy.org](http://www.stratigraphy.org)). We use the following abbreviations to describe the river valleys: N<sub>1</sub> – Miocene, N<sub>1</sub><sup>3</sup> – Late Miocene, N<sub>2</sub> – Pliocene,

N<sub>2</sub><sup>1</sup> – Early Pliocene (Zanclean), N<sub>2</sub><sup>2</sup> – Late Pliocene (Piacenzian), Q<sub>1</sub><sup>1</sup> – Gelasian, Q<sub>1</sub><sup>2</sup> – Calabrian, Q<sub>2</sub> – Middle Pleistocene, Q<sub>2</sub><sup>1</sup> – early Middle Pleistocene, Q<sub>2</sub><sup>2</sup> – late Middle Pleistocene, Q<sub>3</sub> – Late Pleistocene, Q<sub>3</sub><sup>1</sup> – early Late Pleistocene, Q<sub>3</sub><sup>2</sup> – late Late Pleistocene, Q<sub>4</sub> – Holocene, H – altitude of terrace a.s.l., h – elevation above the river water level, M – total thickness of gravel, M' – thickness of alluvium observed in outcrops, m – thickness of the upper fine-grained part of the alluvium, and s – site of observation.

### 2. Regional background

The region of study occupies the northwestern and northern Arabian Plate within Syria. The plate is bordered from the west by the Dead Sea Transform (DST). The recent pattern of the Syrian–Lebanese part of the DST originated at 3.4–4 Ma (Trifonov et al., 1991; Barazangi et al., 1993; Rukieh et al., 2005), or at ~3.7 Ma (Westaway et al., 2006). The East Anatolian fault zone (EAFZ) originated along the north-western margin of the plate at around the same time (Rukieh et al., 2005), or at the end of the Miocene (N<sub>1</sub><sup>3</sup>) (Westaway, 2004). The northern part of the plate is the

\* Corresponding author.

E-mail addresses: [trifonov@ginras.ru](mailto:trifonov@ginras.ru), [vgtrifonov@yandex.ru](mailto:vgtrifonov@yandex.ru) (V.G. Trifonov), [simak2001@mail.ru](mailto:simak2001@mail.ru) (A.N. Simakova).

northwestern termination of the Mesopotamian Foredeep. Its northern part is deformed by the Marginal Folds of Turkey (Ilhan, 1974). These are bounded to the north by the Bitlis (Eastern Taurus) Thrust, corresponding to the Neo-Tethys suture (Robertson, 2000; Robertson et al., 2004). The fold-thrust Palmyride belt adjoins the termination of the Foredeep in the west. The DST, the EAFZ and the Palmyrides border the platformal Aleppo Block (Fig. 1). Its south-eastern boundary is marked by the Rasafeh–El-Faid fault

zone that probably continues the reverse-sinistral Serghaya fault to the NE (Trifonov et al., 2012).

The Lebanon Range in the south and the Coastal Range in the north occupy the dominate part of Lebanon and northwest Syria. These ranges began to rise as marginal anticlines of the Arabian Plate in the Miocene when the northern DST follows Roum Fault and farther along the continental slope of the Mediterranean (Trifonov et al., 1991; Rukieh et al., 2005). The El-Kabir Basin with

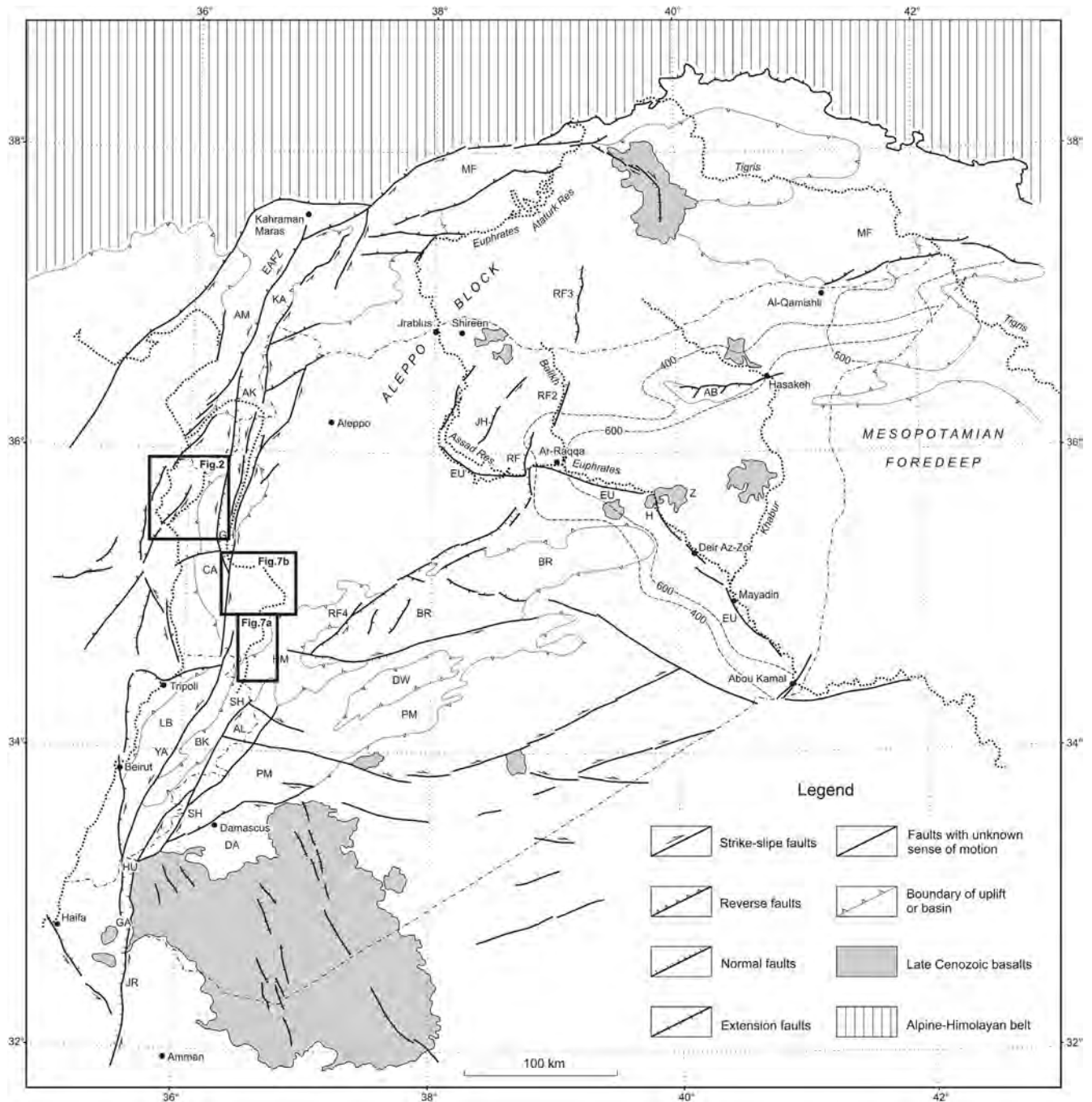


**Fig. 1.** Late Pliocene–Quaternary (the last ~3.5 Ma) tectonic features of the northern part of the Arabian plate. The 400-m and 600-m Miocene isopachs and the 500-m Pliocene isopach demonstrate the structure of the Mesopotamian Foredeep. Contours of Figs. 2 and 7 are shown (after Trifonov et al., 2012, with additions). Uplifted anticline zones: AB, Abdel Aziz; AL, Antilebanon; BR, Bishri, the Northern Palmyrides; CA, Coastal of Syria; LB, Lebanon; MF, Marginal Folds of Turkey; PM, Southern Palmyrides. Faults and fault zones: AM, Amanos, a segment of the EAFZ; EAFZ, East Anatolian; EU, Euphrates; JH, Beer Jabel–Heimer Kabir; JR, Jordanian, a segment of the DST; RF, Rasafeh–Faid and its continuation (RF2, RF3 and RF4); SH, Serghaya; YA, Yammuneh, a segment of the DST. Basins: AK, Amik; BK, Bekkaa syncline; DA, Damascus; DW, Ad Daw; GA, Galilee Sea pull-apart basin of the Dead Sea Transform (DST); GH, El Ghab pull-apart basin of the DST; HM, Homs; HU, Hula pull-apart basin of the DST; KA, Karasu graben. Basaltic fields: H, Halabiyeh; Z, Zalabiyeh.

the Lattaqieh sinistral–reverse fault in the north–western side limited the Coastal anticline to the north. After the structural reorganization dated to 3.4–4 Ma, the Yammuneh and El Ghab faults intersected the anticlines, but they continued to rise even more intensively than before (Gomez et al., 2006; Trifonov et al., 2011). The Lebanon Range rose up to 3 km and the Coastal Range, up to 1.6 km. The uplift of the Coastal Range spread into the onshore part of the El-Kabir Basin and the Bassith Block to the NW of it. The axial part of the Syrian termination of the Mesopotamian Foredeep was situated in the Miocene in its southern part, but it moved in the Pliocene to the north, close to the rising Marginal Folds of Turkey (Rukieh et al., 2005). Only residual depressions with sparse fine-grained sedimentation remained in the south where the Euphrates valley spread later (Trifonov et al., 2012).

Five fluvial terraces as well as recent channel and floodplain were identified in the recent Euphrates, Orontes, and El-Kabir valleys. The youngest deposits composing the terrace basements or the areas where the terrace were incised, are  $N_2$  (Pliocene) in the El-Kabir valley,  $N_2$  or  $Q_1^2$  (Calabrian) in the Orontes and  $N_2^1$  (Early Pliocene) in the Euphrates. Similar numbers and structural position of the terraces in different valleys were arguments to correlate the terraces and to date them to different parts of Pleistocene (not older than  $Q_1^2$ ) and Early Holocene (Ponikarov et al., 1967; Besançon et al., 1977, 1978; Copeland and Hours, 1978, 1993; Besançon, 1981; Besançon and Sanlaville, 1981, 1993; Copeland, 1981; Sanlaville, 1979, 1981). The further studies in the El-Kabir and Orontes valleys confirmed this stratigraphy by additional data (Dodonov et al., 1993; Devyatkin and Dodonov, 2000). Important new data on structure and evolution of the El-Kabir and especially Orontes valleys were represented by Bridgland et al. (2003, 2008, 2012). Bridgland and Westaway (2008) estimated a tectonic uplift and a role of climatic fluctuations in formation of the Orontes terraces in the worldwide context. At the same time, the K–Ar and Ar–Ar dating of basalts covering the Euphrates terraces in the Halabiyeh and Zalabiyeh–Kursa lava field areas and near the village of Ayash proved that the Euphrates terraces occupied the longer time interval than the Orontes and El-Kabir terraces (Sharkov et al., 1998; Sharkov, 2000; Demir et al., 2007; Trifonov et al., 2011). The ages were determined as  $\sim 2.7$  Ma for the basalts on the terrace IV,  $\sim 2.12$  Ma for basalts on the terrace III<sup>b</sup>, 0.7–0.8 Ma for the basalts on the terrace II, and  $\sim 0.4$  Ma for basalts on the terrace I. The Early Paleolithic finds in the terrace III<sup>a</sup> alluvium were attributed to the Khattabian industry, correlated with the Oldowan culture and dated as early  $Q_1^2$  (Calabrian) (Copeland, 2004; Demir et al., 2007, 2008). The established older ages of the Euphrates terraces showed the necessity of more detailed chronological correlation of terraces of large rivers in Syria.

### 3. Methods

The altitudes of the individual terraces have mainly been estimated by leveling above the rivers using a handheld level. Possible errors range from 20–30 cm to 1 m for the terraces situated near the river, but could increase up to  $\pm 2$  m for the terrace localities situated several kilometers farther from the river. In these cases, we controlled the results using a combination of GPS measurements, data of the 3" model of topography SRTM (Shuttle Radar Topography Mission) and by leveling relative to the trig points. The individual terraces were differentiated by field observations. Their correlation along the valley was carried out by field mapping and the analysis of the SRTM data. The geographic coordinates of all sites of field observations were determined by GPS technique and the sites were placed on the SRTM model.

We dated the terraces by using radio-isotopic, magneto-stratigraphic, paleontological, and archaeological methods, coupled with

information on the local sequences and the altitudes of the terraces in the part of the valley studied. We also tried to correlate the terraces with the MIS stages. We used magneto-stratigraphic method only to separate deposits of the Brunhes and Matuyama paleomagnetic epochs in principal sections (the El-Kabir terrace IV near the village of Jinndiriyeh and the Euphrates terrace II near the village of Ayash). The standard technique of successive thermal magnetic cleaning up to temperature of 680 °C was used to estimate the residual magnetic polarity. Attributing of archaeological finds was based on the subdivision of the Acheulian sequence of Syria into the Early, Middle, Late, Late Evolved, and Final Acheulian (Hours, 1981; Muhesen, 1985; Copeland and Hours, 1993). The Early Acheulian industry (choppers, picks, and rare crude bifaces) from Ubeidiya, Southern Levant was dated to  $\sim 1.4$  Ma (Tchernov, 1999). In the Middle Acheulian there were two industrial traditions. The inland sites such as Latamne ( $\sim 1$  Ma) in the Orontes valley contain choppers, picks and lanceolate bifaces, whereas in the seaside sites (El Kabir valley) amygdaloidal and ovate bifaces prevail. The second tradition developed in the Late Acheulian (late Middle Pleistocene) distinguished for thinner and more refined ovate and cordiform bifaces as well as for the appearance of the Levallois technique. In the closing stages of Acheulian both the bifaces and Levallois products tend to be smaller and more perfectly fashioned. The principal question for using archaeological and paleontological finds for terrace dating is whether the finds were re-sedimented or not. Because the archeological and paleontological finds were made in alluvium, all had been moved by water. The artifacts from the El-Kabir terrace III Rondo and the Euphrates terrace II near the Ayash demonstrate signs of weathering and erosion. Nevertheless, the majority of finds are sufficiently preserved to consider that they belong to approximately the same time interval as the enclosing deposits, although there are some exceptions, for example, a position of mammal fossils in the Sharia quarry in the town of Hama (Besançon et al., 1978). Lenticular alternations of pebbles and sands represent the channel deposits, which now make up much of the terrace deposits. In contrast, the recent flood plains are mainly made up of 1–5 m thick silts, loams and clays that dominate the upper part of the terrace sections. The presence of fine-grained material in the terrace surfaces indicates an absence of significant erosion.

### 4. The Nahr El-Kabir valley

The source of Nahr El-Kabir (El-Kabir River) is situated in the northern Coastal Range (the Bassit Block). This  $\sim 70$ -km long river flows along the El-Kabir Basin to the Mediterranean and reaches it to the south of the city of Lattaqieh (Fig. 2). Formation of the Nahr El-Kabir fluvial terraces was preceded by marine sedimentation in the El-Kabir Basin, which continued throughout the entire Neogene and a part of Early Pleistocene, according to the nannoplankton data (Devyatkin and Dodonov, 2000). In sections of Msherpheh, Mardido and Al-Quatriya in the south of the basin, the Mediterranean scale zones were identified (Rio et al., 1991): *Discoaster pentaradiatus* ( $N_2^2$ ), *Discoaster brouweri* ( $Q_1^1$ ), and the unit with *Gephyrocapsa oceanica* and *Helicosphaera sellii*, characteristic for  $Q_1^2$ . The latter composes the upper 30 m of the sections, has normal magnetic polarity (in contrast to the reverse polarity of the lower sediments) and probably belongs to the Olduvai episode (Devyatkin et al., 1996).

Five fluvial terraces are identified in the El-Kabir valley, the terraces II and III being represented by two sublevels (Table 1). The highest terrace V Sitt Markho ( $h \approx 130$  m) was identified at the single site near the eponymous village. The Early Acheulian artifacts were found within the terrace V alluvium (Besançon et al., 1977; Sanlaville, 1979; Muhesen, 1985).

**Table 1**  
Height of the Nahr El Kabir terraces in both sides of the Lattaqieh fault.

N of terrace	Age	NW side of the fault: height, m/site of observation	SE side of the fault: height, m/site of observation	The fault	
				Offset, m	Rate of motion, mm/ky
I	Q <sub>4</sub> ; <14 ka	4/60	4–6/62; 6/64	0	?
II <sup>a</sup>	Q <sub>3</sub> ; ~90–130 ka/80 ka	20–25/534; 19/59; 15/61; 20–25/60	7/646; 11/711; 9–10/645; 13/535; 10/637; 17/712; 12/62; 10/66	9 ± 2	~100
II <sup>b</sup>	Q <sub>3</sub> ; ~90–130 ka/80 ka	41/691	24/711a; 27–28/645; 24–25/644; 34/642; 32/62; 35/64; ~35/65; 38/66	10 ± 3	
III <sup>a</sup>	Q <sub>2</sub> <sup>2</sup> ; ~280–420 ka/~270 ka	81–82/688; 65–75/633 = 55; 70–75/61	53/643; 59/631a; 47/714 = 54a; 48/713	22 ± 4	~70
III <sup>b</sup>	Q <sub>2</sub> <sup>2</sup> ; ~280–420 ka/~270 ka	94/634; 94–100/630 = 54 (Roudo); ~90/58; 90/63	72/638; 71/62; 73/66	21 ± 2	
IV	Q <sub>1</sub> <sup>1</sup> ; ~620–480 ka/~430 ka	112/636; 120/629 (Jinndiriyeh)	80–90/Hennadi; 95/62; 108/66	16 ± 6	0
V	Q <sub>1</sub> <sup>1</sup> ; ~620–480 ka/~430 ka	~130/Sitt Markho*; 120–130/Baqsa*			

In columns 2: age of sedimentation/age of following incision. In columns 3 and 4: height of terrace/site of observation. Height of marine terraces is shown by *italics*. \* is reference to (Devyatkin et al., 1996; Devyatkin and Dodonov, 2000). The rates of motion on the Lattaqieh fault are related to the time interval between the beginning of incision into the terrace alluvium and the beginning of incision into the younger terrace alluvium.

Terrace IV was studied in detail near the village of Jinndiriyeh (s 629, N35.5866°, E35.8799°, *h* ≈ 120 m, *M* ≈ 35 m). A base of the terrace consists of the N<sub>2</sub> grey clays as thick as 25 m; according to the nannoplankton composition (*Reticulofenestra pseudo-*

*umbilica* and higher *Discoaster tamalis*) and normal magnetic polarity, the age of the clays is 3.8–3.4 Ma (Devyatkin et al., 1996). The following section lies above an erosional contact (upwards) (Fig. 3):

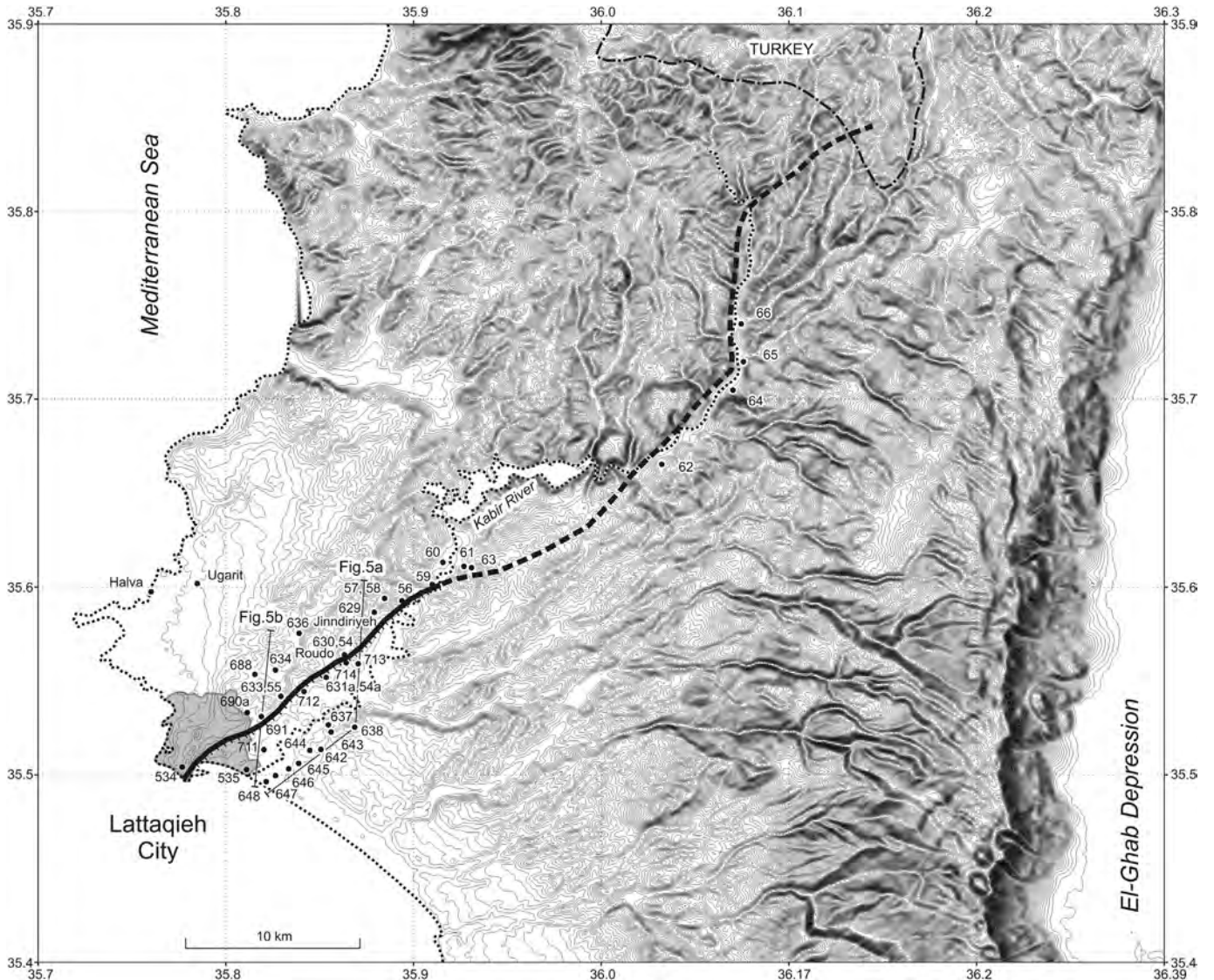


**Fig. 2.** The Nahr El-Kabir valley. The map demonstrates isohypses with the 10-m interval according to the Shuttle Radar Topography Mission (SRTM) data and the location of Lattaqieh Late Cenozoic fault and sites of our observations. Hachures on fault lines are directed to downthrown sides. The approximate position of the profiles 5a and 5b is shown.

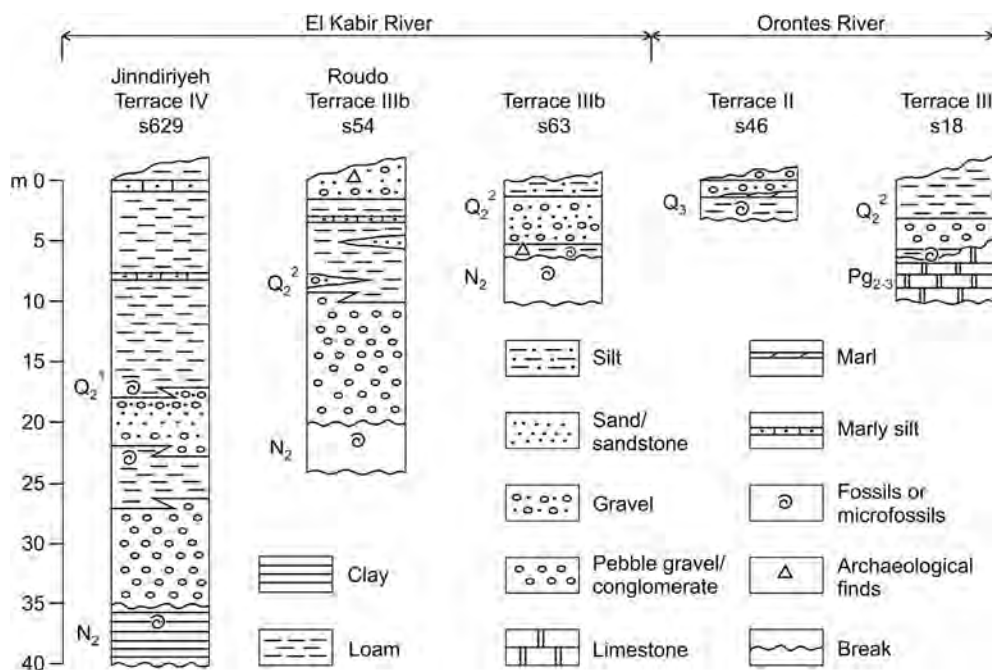


Fig. 3. Sections of terraces of the Nahr El-Kabir valley: (s 629) the terrace IV Jinndiriyeh; (s 54 = 630) the terrace III<sup>b</sup> Roudo; and (s 63) the terrace III<sup>b</sup>; and of the Orontes valley: (s 46) the terrace II and (s 18) the terrace III.

1. Lens-type alternation of pebbles of different size and rounding. The bottom is situated ~80 m above the river water level. The thickness is up to 10 m.
2. Silt and soft fine-grained sandstone. Fragments of mollusks in the upper part. Up to 5 m.
3. Lens-type alternation of soft sandstones and small-pebble conglomerate. 5 ± 2 m.
4. Silt and soft fine-grained sandstone. Thin interbeds of hard carbonate silt, the thickest interbed (5–10 cm) is situated in the upper part of the unit. Fragments of mollusks in the lower part. At the same level (~100 m above the river), the lower mandible of the Middle Pleistocene rhinoceros *Stephanorhinus hemitoechus* (Falconer, 1868) was found (determination of V.Yu. Reshetov; Devyatkin and Dodonov, 2000). The thickness is ~20 m.

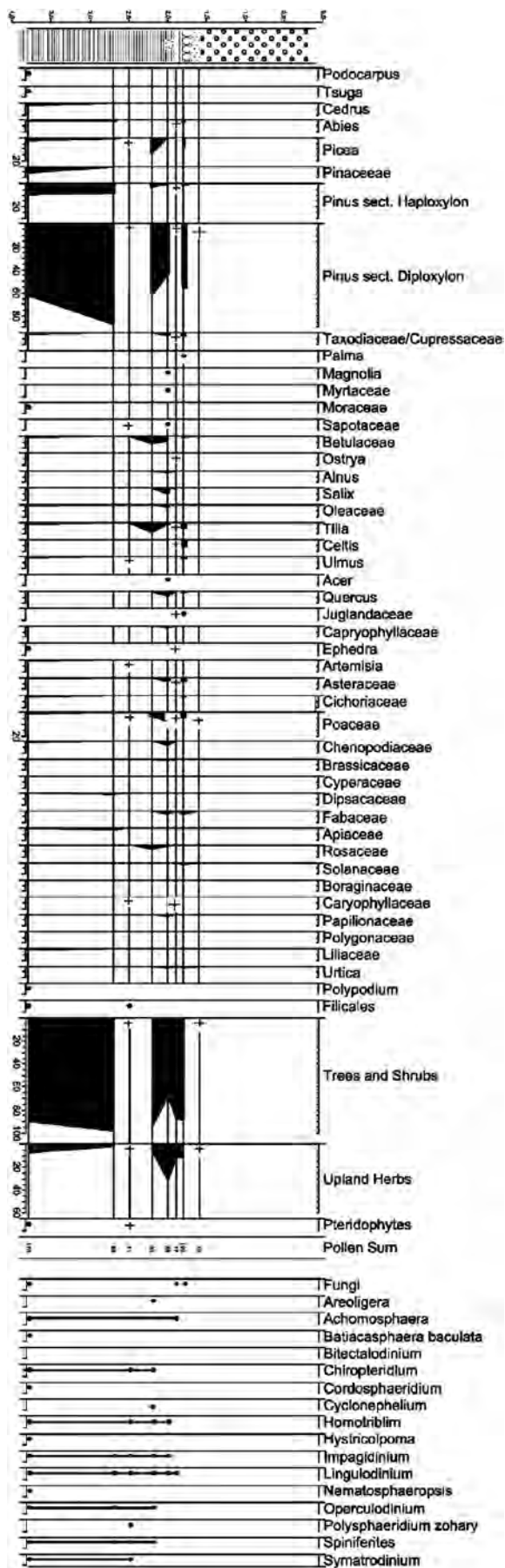
Palynological spectrum of the alluvial cover of the terrace shows approximately equal values of pollen of arboreal and herbaceous plants (Simakova, 1993). The pollen of *Pinus* dominates in the arboreal-shrub group (up to 56%); *Quercus*, *Acer*, and *Carpinus* are present among the broad-leaved group. Changes of the pollen composition upwards demonstrates climatic change from rather humid to more arid conditions.

Terrace III<sup>b</sup> was studied near the villages of Roudo (s 54 = 630, N35.5628°, E35.8638°, h = 94–100 m; M ≈ 24 m) and Jabryoun (s 63, N35.7074°, E36.0675°, h ≈ 90 m, M ≈ 6 m). The s 54 section from the bottom upwards (Fig. 3) shows:

1. Base of the terrace: bedded grey clayish silt with Pliocene mollusca. Visible thickness reaches several meters.
2. Conglomerate with sand lenses; 8 m.
3. Silt with lenses of sand and gravel and hard carbonate silt interbeds; 15 m.
4. Pebbles, sand and silt with soil cover; ≥1 m. We have found weakly eroded artifacts within and in the surface of the layer 4. They are attributed to the end of Middle Acheulian or Late Acheulian.

The s 63 section demonstrates from the bottom upwards (Fig. 3):

1. Brownish-grey clay; up to 2 m (visible). The arboreal pollen dominates in palynological spectra (up to 90–97%). Conifers are represented by pollen of *Pinus* sg. *Dyploxylon*, *P. sg. Haploxylon*, *Podocarpus*, *Tsuga*, *Cedrus*, *Abies*, and *Picea*. Pollen of *Sapotaceae*, *Oleaceae*, *Betulaceae*, *Moraceae*, *Tilia*, and *Ulmus* characterize the deciduous group. The herbaceous plants are represented by pollen of *Asteraceae*, *Poaceae*, *Chenopodiaceae*, *Apiaceae*, *Dipsacaceae*, and *Ephedra* (Fig. 4). Spectra demonstrate the predominance of the coniferous–broad-leaved forests with small areas of meadow-steppe vegetation. These spectra are similar to pollen spectra from the Pliocene clays of the Jinndiriyeh terrace (Simakova, 1993; Devyatkin et al., 1996). *Spiniferites* spp., *Operculodinium* spp., *Lingulodinium machaerophorum*, and *Hystrichokolpoma* spp. dominate in the dinoflagellate group. According to L.A. Golovina (Simakova et al., 2012), the nannofossil assemblage includes abundant *Sphenolithus abies*, *S. moriformis*, *Coccolithus pelagicus*, *Discoaster brouweri*, *D. pentaradiatus*, *D. surculus*, *Pontosphaera multipora*, *P. discopora*, *Rhabdosphaera clavigera*, *Reticulofenestra pseudumbilica*, small *Reticulofenestra*, *Scyphosphaera* sp., *Dictyococcites* spp., and a few *Discoaster tamalis*. This assemblage of nanoplankton corresponds to the MNN14/15 Zone according to calcareous nannofossil biostratigraphic scheme for the Pliocene–Pleistocene of the Mediterranean (Martini, 1971; Rio et al., 1991). Thus, the age of the clays at the base of the alluvial terrace of the Nahr El-Kabir River is Early Pliocene by pollen and dinocysts data; according to nanoplankton data, it is 4.2–3.8 Ma and corresponds to the Zanclean.
2. Brownish-grey loam with fine (up to 6 cm) carbonate layer in the upper part; 0.7 m. The Acheulian hand-axe was found within the unit. Typical forms of the maquis groups (*Myrtaceae*, *Ostrya*, *Alnus*, *Salix*) dominate in the palynological spectrum. This is similar to the Middle Pleistocene spectra of Western Syria (Simakova, 1993). At the same time, rare Late Pliocene



nannoplankton and dinoflagellates were found. The latter are *Impagidium patulum* and *Homotriblium* spp., including *H. vellum* which disappeared in the Late Pliocene. Thus, layer 2 belongs to the terrace cover and was formed by recycling of the Pliocene deposits in continental or shallow-water conditions; there is a hidden erosional contact between the base of the terrace (unit 1) and layer 2. The hand-axe found in layer 2 may be attributed to Middle or Late Acheulian.

3. Sandstone and gravel with lenses of small-pebble conglomerate; cross-bedding is characteristic; up to 4 m.
4. Loam and silt with rare pebbles and fine layers, enriched by carbonate; 1.5–2 m; very rare pollen of pines and grasses.

A section of the accumulative terrace III<sup>a</sup> was described in the Lattaqieh fault zone near the village of Jabryoun (s 61, N35.6093°, E35.9245°,  $h = 70\text{--}75$  m,  $M' \approx 70$  m). The section demonstrates from the bottom upwards (Fig. 3):

1. Coarse sandstone and gravel with abundant loam matrix; a significant portion of debris consists of ophiolite and radiolarite that are exposed in the northwestern side of the Lattaqieh Fault. Visible thickness is ~10 m.
2. Thick (~40 m) unit with alternating pebbles and finer-grained material to silt. The pebbles are small and medium size and vary in roundness.
3. Horizontally bedded silt of probable lacustrine origin, with carbonate interbeds and rare lenses of coarser material; 10–15 m.
4. Lens-type alternation of sandstone, gravel, and well-rounded small-size conglomerate; 5–10 m. The unit is covered by a recent cultural layer of a ploughed field.

In terrace II<sup>b</sup> section (s 64 and s 65,  $h = 35$  m), the 1–2-m thick (up to 4 m in swells) well-rounded pebble gravel covers the Helvetian limestone. A flint tool produced by the Levallois technique typical for the Middle Paleolithic was found in the upper part of the s 65 alluvium (N35.7197°, E36.0759°). A section of terrace II<sup>a</sup> is exposed in s 60 (N35.6130°, E35.9157°,  $h = 20\text{--}25$  m,  $M' \approx 12$  m). The lower part of the section consists of pebble gravel with sand lenses; cross-bedding is characteristic. The upper part of the section consists of silt with small lenses of gravel and the sand layer at the bottom. Archaeological finds in the lower part of the upper unit are probably related to the Middle Paleolithic, but could be younger. Thickness of the pebble unit reaches ~10 m and decreases away from the El-Kabir River. Thickness of the silt unit increases in the same direction up to ~6 m. Terrace I (s 62 and s 64,  $h = 4\text{--}6$  m) consists of pebble gravel, usually covered by silt. Bedrock is often exposed in the terrace base.

The youngest marine sediments in the El-Kabir Basin are dated to late Early Pleistocene. Thus, the river valley is younger. Early Acheulian artifacts are present in the terrace V Sitt Marho alluvium (Besançon et al., 1977; Sanlaville, 1979; Muhesen, 1985). Similar artefacts have been found within the Euphrates terrace II alluvium, which shows reverse magnetic polarity and is covered by basalt with normal magnetic polarity and K–Ar dates of 0.7–0.8 Ma. This indicates an age of late Early Pleistocene.

The lower mandible of rhinoceros from the terrace IV Jindiriyeh alluvium with normal magnetic polarity was dated as the Middle Pleistocene (Devyatkin and Dodonov, 2000). The pollen spectra of the Jinndiriyeh alluvium is characteristic for the Middle Pleistocene of Western Syria (Simakova, 1993). These data and the

Fig. 4. Pollen diagram of the section (s 63) of the Nahr El-Kabir terrace IV.

position of the terrace IV between the terraces V and III<sup>b</sup> estimate the terrace IV age as Q<sub>2</sub> (probably Q<sub>2</sub><sup>1</sup>).

The finds from the upper layer of the terrace III<sup>b</sup> Roudo have been attributed to the end of Middle Acheulian or Late Acheulian. Previous researchers estimated finds in the same layer as Late Acheulian (Sanlaville, 1979; Besançon, 1981a,b; Muhesen, 1985) or Middle Acheulian (Devyatkin and Dodonov, 2000). The Acheulian complex seems to be younger than the Latamne one. The hand-axe from unit 3 of s 63 may be attributed to Middle or Late Acheulian also. Palynological spectra from unit 3 of s 63 are characteristic for Middle Pleistocene. From these data, we estimate the terrace III<sup>b</sup> age as late Middle Pleistocene.

Archaeological finds in the terraces II<sup>b</sup> (s 65) and II<sup>a</sup> (s 60) alluvium are probably related to the Middle Paleolithic, although the artefacts from s 60 could be younger. These data indicate that terraces II<sup>b</sup> and II<sup>a</sup> could correspond to Late Pleistocene (probably to early Late Pleistocene). We date terrace I as Early Holocene, because it transforms in the Nahr El-Kabir mouth into the coastal-marine terrace I. A mollusk from this terrace is dated by the <sup>230</sup>Th/U technique as 7.8 ± 1.3 ka (Dodonov et al., 2008).

The Lattaqieh Fault strikes along the Nahr El-Kabir and usually coincides with the river channel or cuts the upper terraces of the

northwestern side of the valley. Continuation of the fault activity in the Quaternary is registered by higher terraces on the northwestern side of the valley above those on the southeastern side (Fig. 5a,b and 6; Table 1). Uplift of the northwestern side of the fault is expressed also by erosional or abrasional (near the sea) terraces with very thin pebble cover (ss 534, 633 = 55, 634, 636, 688 and 691), in contrast to the southeastern side terraces that are covered by thick sections of alluvium or coastal-marine sediments. The height difference on opposing sides of the fault reaches ~20 m for terraces IV, III<sup>b</sup> and III<sup>a</sup> and ~10 m for terraces II<sup>b</sup> and II<sup>a</sup>. Offset of the terrace I was not found. This means that the Quaternary movements on the fault began at the end of Middle Pleistocene and were essentially reduced in Holocene. The fault continues to be active, as shown by strong historical earthquakes in its zone and moderate instrumental earthquakes in the off-shore southwestern continuation of the fault (Sbeinati et al., 2005; Trifonov, 2012).

### 5. The Orontes River valley

The source of the Orontes (Al-Asis) River is situated within the Bekkaa valley-syncline between the Lebanon and Anti-Lebanon ranges-anticlines. In Syria, the river crosses different structural

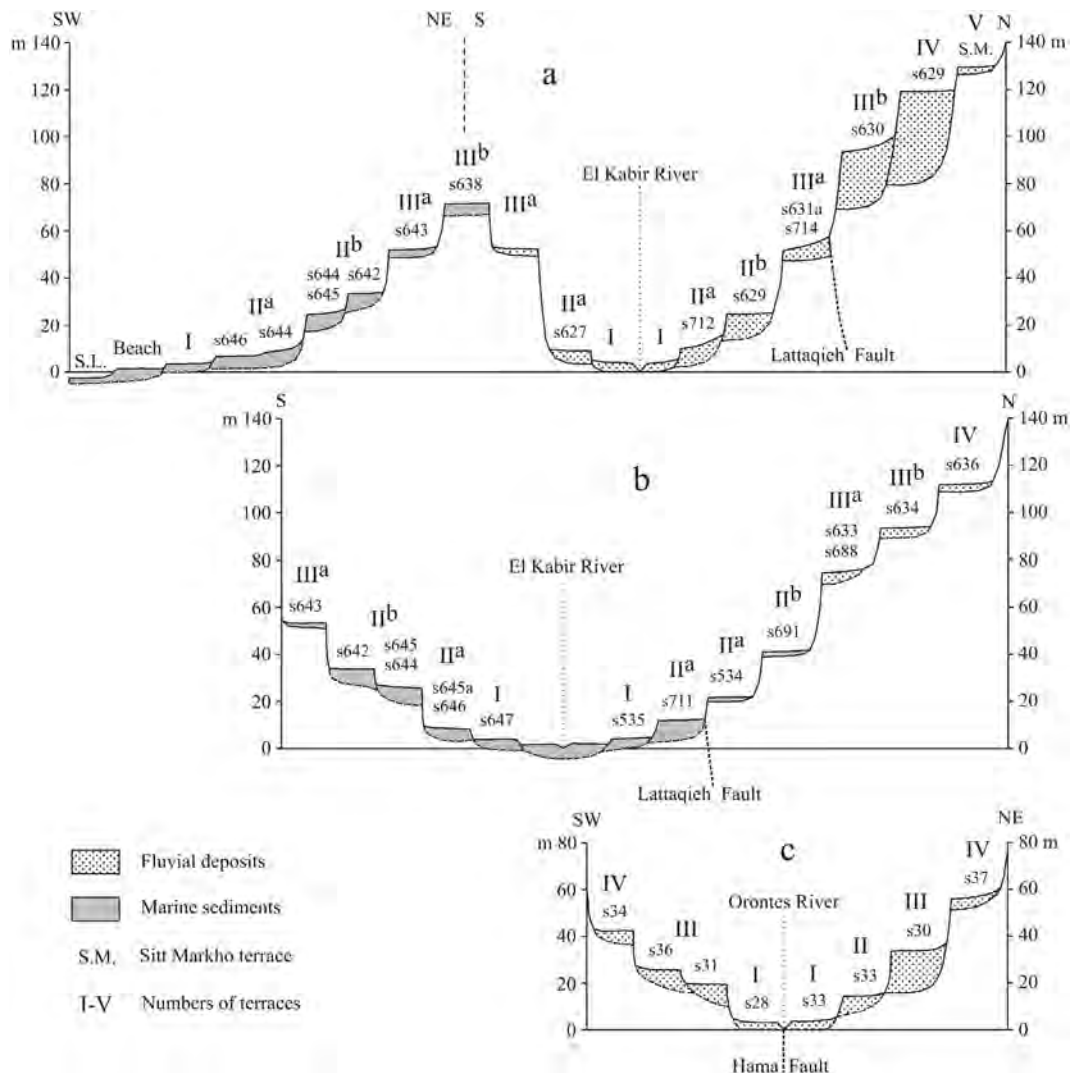


Fig. 5. Principal geomorphological profiles across river valleys: a, the N–S-trending profile across the El-Kabir valley via the Jinndiriyeh and Rudo terraces, continued to the SW along the southern slope of the valley; b, the N–S-trending profile across the El-Kabir valley via the eastern side of the city of Lattaqieh; c, the SW–NE trending profile across the Orontes valley near the village of Khattab. The approximate position of the profiles is shown in Figs. 2 and 7.

elements of the Aleppo Block (segments A–E in Fig. 7) and continues downstream to the El-Ghab pull-apart basin of the DST. The river flows to the western Amik Basin near the town of Antioch (Antakia), turns to the SW along the EAFZ, and reaches the Mediterranean.

The segment A of the Orontes valley crosses the Homs Basin. Because of damming by the  $N_1^3-N_2^1$  (Late Miocene–Early Pliocene) Shin Plateau basalts (Trifonov et al., 2011), incision is small in the upper part of the valley and increases only to the north of the Buheiret Qattinen Lake, where the Orontes rounds the plateau from the east. Three lower terraces are identified (Table 2). They are composed of alluvium or have Pliocene marls as a base and are identified, correspondingly, to the Al-Hauz, Arjun and Tir M'ala terraces of Bridgland et al. (2003). All rise to the north: terrace I – from ~1.5 m (ss 45 and 46) to ~4 m (ss 6 and 7), terrace II – from ~7 m (ss 46 and 52) to ~10 m (ss 50, 5 and 6), and terrace III – from ~13 m to ~27 m (ss 52 and 6). In s 46 (N34.5775°, E36.5462°, see Fig. 3), the following section of terrace II is exposed from the bottom upwards:

plain relative to all Orontes terraces. Ponikarov et al. (1967; Geological Map of Syria, 1964) dated these deposits as Villafranchian, i.e.,  $Q_1^1$  and early  $Q_1^2$ . The section near the road Damascus–Homs to the south of the Rastan Dam (s 12, N34.9249°, E36.7396°,  $h \approx 80$  m,  $M \approx 8$  m), from the bottom upwards (Fig. 8) is:

1. Cretaceous limestone and marls; visible thickness reaches several meters.
2. Basaltic flow of the Shin series ( $N_1^3-N_2^1$ , Trifonov et al., 2011). It is present only in the southern part of the outcrop, where thickness of the basalt reaches 1.5 m. The basalts of the upper part of the flow are pillow-lavas, i.e., they hardened in water. The basalts feather out to the north and continue as single “pillows” (up to 0.5–0.8 m along the layer) as well as angular fragments of the basalt within the conglomerate with carbonate matrix, similar to unit 3.
3. Conglomerates with carbonate matrix, including interbeds of calcareous sandstone and sandy limestone; total thickness is up to 6 m. Surfaces of weathering and erosion are observed within

**Table 2**  
Height of the Orontes terraces in different segments of the valley.

Segment of the valley	Height of terraces, m (and sites, s)				Basic surface
	I	II	III	IV	
A	1–1.5 (s 46); ~3.5 (s 47); 2–4 (s 51); 1.5–2 (s 52); 1.5–2 (s 4); ~2 (s 5); 3.5–5 (s 6); ~4 (s 7)	6–7 (s 46); 5.5 (s 47); ~10 (s 50); ~7 (s 52); 9–10 (s 5); ~10 (s 6); ~13 (s 7)	12–13 (s 52); ~27 (s 6)		
B	~5 (s 14); ~3.5 (s 17); ~3 (s 18)	15.5–17 (s 14); ~17 (s 17)	~25 (s 17); ~26 (s 18)	45–50 (s 14)	~80 (s 12); ~100 (s 9)
C	~2.5 (s 8); 3.5–4 (s 11); 2.7–3 (s 19); 2–5 (s 20)	13.5 (s 11); 13.6 (s 19)	~26 (s 11); >20 (s 19); 29 (s 20)	51 (s 20); ~60 (s 21)	
D, NE side of Hama fault	~4 (s 22); ~8 (I <sup>P</sup> , s 22); ~4 (s 23); 3–4 (s 33)	~15 (s 33)	~28 (s 23); ~35 (s 30); ~26 (s 33); 29–30 (s 38)	~49 (s 35); 55–60 (s 37); 50–60 (s 39)	
D, SW side of Hama fault	~3 (s 26); ~3.5 (s 28)		~20 (s 26); ~26 (s 27); 19–20 (s 31); ~20 (s 32); 19–20 (s 35); ~26 (s 36)	~43 (s 28); ~43 (s 34)	
E	~3 (s 43)		~38 (s 42); ~33 (s 43)		

1. Horizontally bedded silt and fine-grains sand. A fragmentary non-mineralized scapula of *Equus* sp. and a molar (m3) of common vole, *Microtus* sp., dated as Late (?) Pleistocene, were found. Observable thickness is up to 2 m.
2. White marl; up to 0.5 m. The marl disappears upstream, eroded by unit 3.
3. Poorly rounded pebbles and gravel; up to 2.5 m. The top of the unit is destroyed by agricultural activity.

Bridgland et al. (2003) described a series of nine higher calcreted (with carbonate cement) terraces on the southeastern side of the Orontes at a distance up to 15 km from the river. Later, they increased their number up to 12, with the altitude of the highest reaching ~180 m above the river level (Bridgland et al., 2012). The Al-Qusayr terrace ( $h = 47$  m) can be correlated with the Latamne terrace IV of the Middle Orontes; the Bwayda Al-Sharqiyya terrace gravel ( $h = 75$  m) is not seen well, but correspond probably to the Quaternary deposits near the Rastan Dam (our s 12; see below). We consider the higher levels of Bridgland et al. (2003, 2012) as the terrace-like steps in the northern end of the Anti-Lebanon Ridge that characterize its uplift, whereas the recent Upper Orontes valley formed within the Homs Basin and only the three lower terraces and probably the Al-Qusayr and Bwayda Al-Sharqiyya ones characterize its uplift.

In segment B, the Orontes flows along the northern side of the Homs Basin. The Lower Quaternary deposits are incised into the rough surface of the Cretaceous carbonates and form the summit

the unit. In the southern part of the outcrop, above the basalts, the conglomerates are incised into the Cretaceous limestone. We identified the conglomerates as a fluvial deposit, but not the Orontes alluvium. The relationships between the basalts and conglomerates demonstrate that the accumulation of conglomerates started during the basaltic eruption, i.e., in the  $N_2$ . The thickness of conglomerates does not increase towards the recent Orontes valley. Probably, the valley was not formed at the time of their accumulation.

Similar unit of horizontally and cross bedding conglomerates with poorly rounded pebbles, carbonate matrix and lens-type interbeds of calcareous sandstone and limestone covers rough surface of the Paleogene limestone in s 9 (N34.9660°, E36.8518°,  $h \approx 100$  m,  $M \approx 6$  m). The pebbles consist of limestone, flint and calcareous-flinty concretions as well as basalt in the lower part. Units s 9 and s 12 probably correspond to the Khattab terrace downstream,  $h \approx 80$  m that represent the higher topographic level for a long distance of the left side of the Middle Orontes (Besançon et al., 1978). Copeland and Hours (1993) described the primitive Khattabian culture of artifacts without hand-axes and argued that it was older than Acheulian industries.

Four terraces are incised into the surface, composed of Cretaceous–Paleogene rocks and the described conglomerate unit (Table 2). They are the terraces I (ss 14, 17 and 18;  $h = 3–5$  m), II (ss 14 and 17;  $h = 15.5–17$  m), III (ss 17 and 18;  $h = 25–26$  m), and IV (s 14;  $h = 45–50$  m). In terrace III (s 18, N34.9540, E36.8202,  $h = 26$  m,

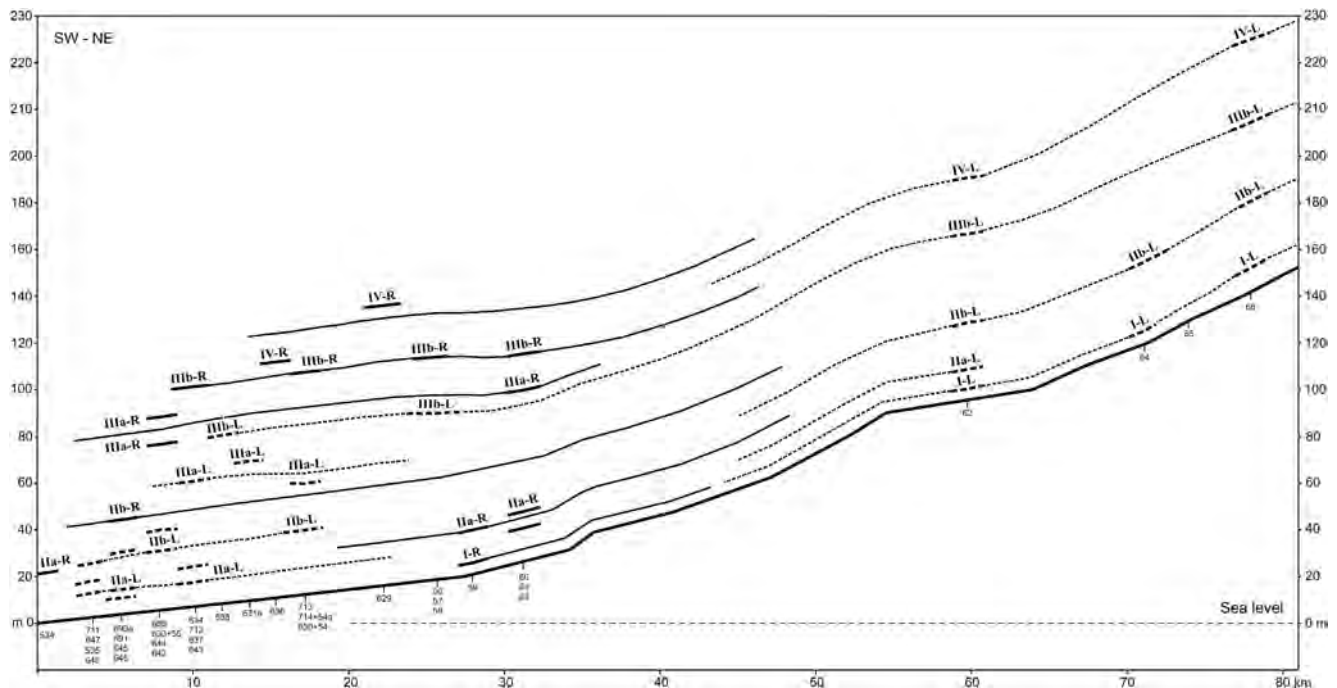


Fig. 6. Geomorphological profile along the Nahr El-Kabir valley, based on combined evidence; “R” is the NW side of the Lattaqieh fault and “L” is the SE side. These sides correspond usually to the right and left banks of the valley.

$M = 6$  m), the following section is exposed from the bottom upwards (Fig. 3):

1. Paleogene limestone. Visible thickness is 2 m.
2. Silt with rare pebbles and a layer of pebbles in the bottom; 0.4 m.
3. A lens of pebbles with silt matrix; 0.1 m.
4. A lens of loam; 0.15 m.
5. Pebble gravel and gravel, often cross-bedding; the pebbles consist of carbonates, flint and basalt; the thickness is up to 2.3 m and decreases to the north where the lower layers feather out due to the rise of the carbonate basement.
6. Loess-like silt and loam with irregular base; 3–5 m.

The pollen abundance varies in the section (Fig. 9). Layer 1 contains sporadic pollen grains (samples 6–8). The arboreal group is characterized by pollen of *Pinus*, *Tilia*, *Ostrya*, *Juglandaceae*, *Betula*, and *Quercus*; the herbaceous plants are represented by pollen of *Asteraceae*, *Chenopodiaceae*, *Caryophyllaceae*, and *Poaceae*. The meadow and steppe plant associations co-occurred in landscapes with small areas of forest vegetation, possibly situated in the river valley. The climate was relatively arid. A more representative pollen spectrum was obtained in layers 3 and 5 (samples 1–4). The arboreal group reaches 25% of the total pollen spectrum. It includes pollen of *Picea*, *Pinus*, *Fagaceae*, *Juglandaceae*, *Liquidambar*, *Buxus*, *Tilia*, and *Tamarix*. The herbaceous group is represented by pollen of *Asteraceae*, *Echonops*, *Plumbaginaceae*, and *Poaceae*. Steppe landscapes dominated, combining with small areas of forest vegetation. The variety of broad-leaved pollen shows that the lower part of the section was accumulated under wetter conditions than the younger one.

In segment C, the Orontes flows to the north, and terraces I, II, III and IV are identified in its banks (ss 8, 10, 11 and 19–21). Height of the upper terraces increases (ss 20 and 21): III – to 29 m and IV – to 51–60 m. In segment D, the Orontes flows to the NW along the Hama fault zone, which is expressed by straight segments of the

valley and offsets of the terrace deposits (Fig. 10). The terraces are represented well near the village of Khattab and downstream to the town of Latamne. The ~15-m thick sedimentary cover of terrace IV is exposed in two quarries in the southwestern margin of the town of Latamne (s 39, N35.3145°, E36.6140°,  $h = 55$ –60 m). The section consists of lens-type alternating rounded pebbles, gravel, sands, and silt. The content of fine-grained material increases in the upper part of the section. We found mammal remains (Fig. 11) within the sand layer in ~12 m below the top of the northwestern quarry, i.e., below the terrace edge. The teeth of horse *Equus ex gr. stenorhis* and astragal bones of *Artiodactyla* are identified that corresponds to the end  $Q_2^1(?)$ – $Q_2$ . Hooijer (1962) reported from a quarry near Latamne: *Stegodon cf. trigonocephalus*, *Elephas trogonterii*, *Equus* sp., *Dicerorhinus cf. hemitoechus*, *Hippopotamus amphibius*, *Orthogonoceros verticornis*, *Camelus* sp., *Antilopidarum* gen. et sp. indet, *Bison cf. priscus*, *Canis cf. aureus*, and *Crocota crocuta*. Perhaps, they were found at the same layer as our finds.

The best exposure of terrace III is situated in the right side of the Orontes River opposite the village of Khattab (s 30, N35.1954°, E36.6877°,  $h \approx 35$  m; s 32,  $h \approx 20$  m). The ~20-m thick terrace alluvium rests on the Paleogene carbonate base and consist of lens-type alternations of pebbles of different sizes, gravel, and sand. Silt and fine-grained sand predominate in the upper 5–7 m of the section. We collected the Acheulian artefacts (Fig. 11) from the terrace III alluvium in s 30 and s 32 (N35.2265°, E36.6634°,  $h \approx 20$  m).

In segment D, the terraces of the northeastern side of the Orontes valley rise above the correlated terraces in the same bank farther to the SW and in the opposite side of the valley (Figs. 5c and 12; Table 2). This indicates uplift of the northeastern side of the fault. The magnitude of the offsets of the terrace I is usually  $\leq 1$  m. The difference of height on different sides of the fault reaches 6–9 m for the terrace III and 7–17 m for the terrace IV. This demonstrates recurrence of the fault movements.

Downstream, in segment E, the Orontes flows to the west and reaches the southern part of the subsiding El-Ghab pull-apart basin

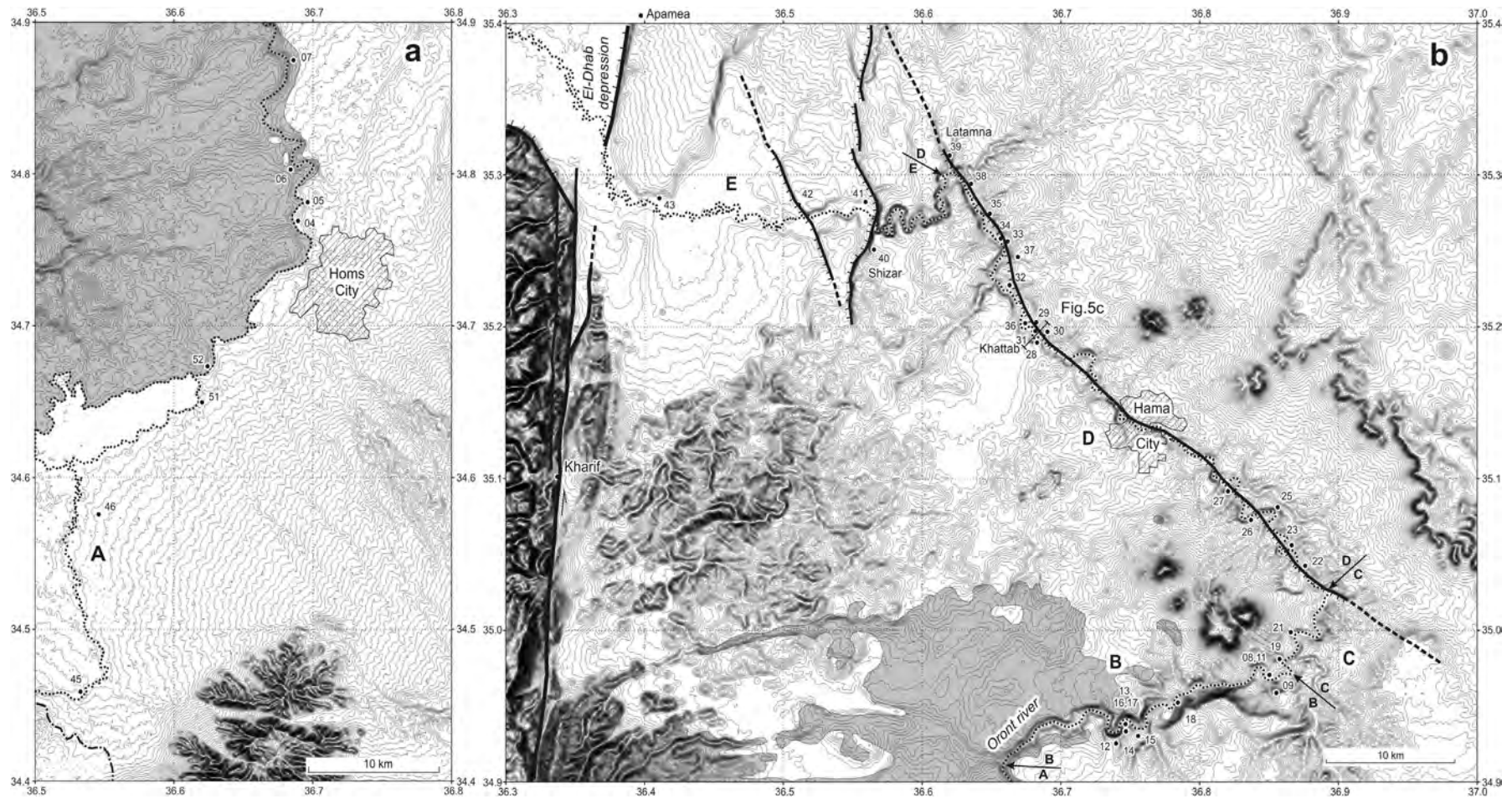


**Fig. 7.** The Orontes River valley. The map demonstrates isohypses with the 10-m interval according to the Shuttle Radar Topography Mission (SRTM) data and the location of Hama and other faults and sites of our observations. Hachures on fault lines are directed to downthrown sides. Arrows show the borders of segments A–E of the valley. The approximate position of the profiles 5c is shown.

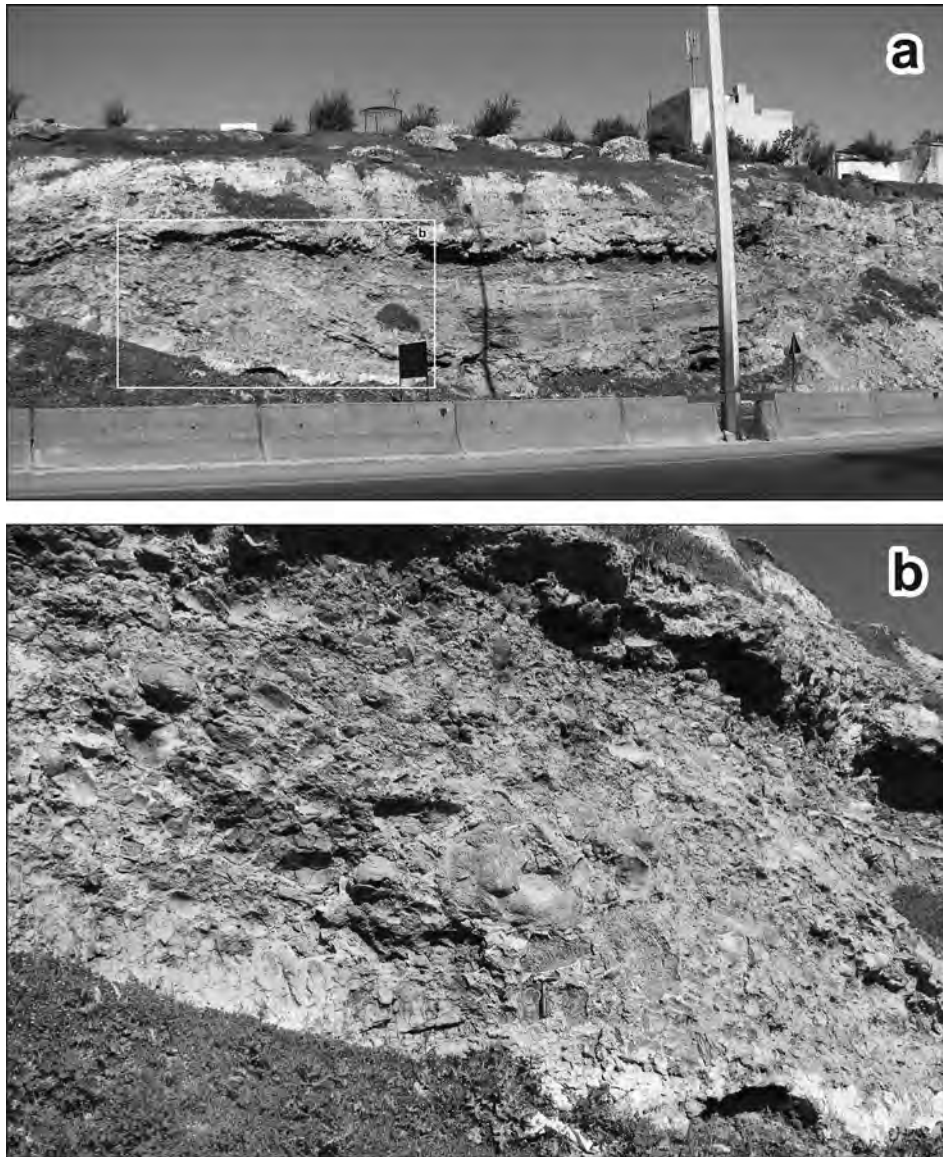


Fig. 8. Excavation of the  $Q_1^2$  section near the road Damascus–Homs to the south of the Rastan Dam (s 12,  $h \approx 80$  m,  $M \approx 8$  m).

where the river terraces feather out. In the village of Chizar (s 40) and downstream (s 42), the Orontes valley is offset by active faults (Fig. 13). Because of the displacement, the height of the terrace III increases from  $\sim 33$  m (s 43) to  $\sim 38$  m (s 42). The fresh offsets on the Chizar Fault are probably related to the 12.08.1157 earthquake with  $M_s = 7.4$  (N35.4° and E36.5°) (Sbeinati et al., 2005; Trifonov, 2012).

The following data are used to estimate an age and environment of the Orontes terrace alluvium. The mammal remains from Hooijer (1962) and later collections, found within the terrace IV, were dated as  $Q_2^1$  (Guérin et al., 1993). The composition of our paleontological collection does not contradict this estimate, with the end of  $Q_1^2$  also conceivable. Devyatkin and Dodonov (2000) described the section in the Miramil quarry that likely corresponds to our northwestern quarry. They reported finds of the Middle Acheulian hand-axes in the depth of 8 m from the quarry top. They also reported thermoluminescence dates of fine-grained material from depths of 5.5 m and 8.5 m from the top of the quarry. Dating was carried out by O.A. Kulikov from the Chemical Faculty of the Moscow State Lomonosov's University and gave, correspondingly,  $324 \pm 65$  ka and  $567 \pm 42$  ka. Clark (1967, 1968) reported the Middle Acheulian finds

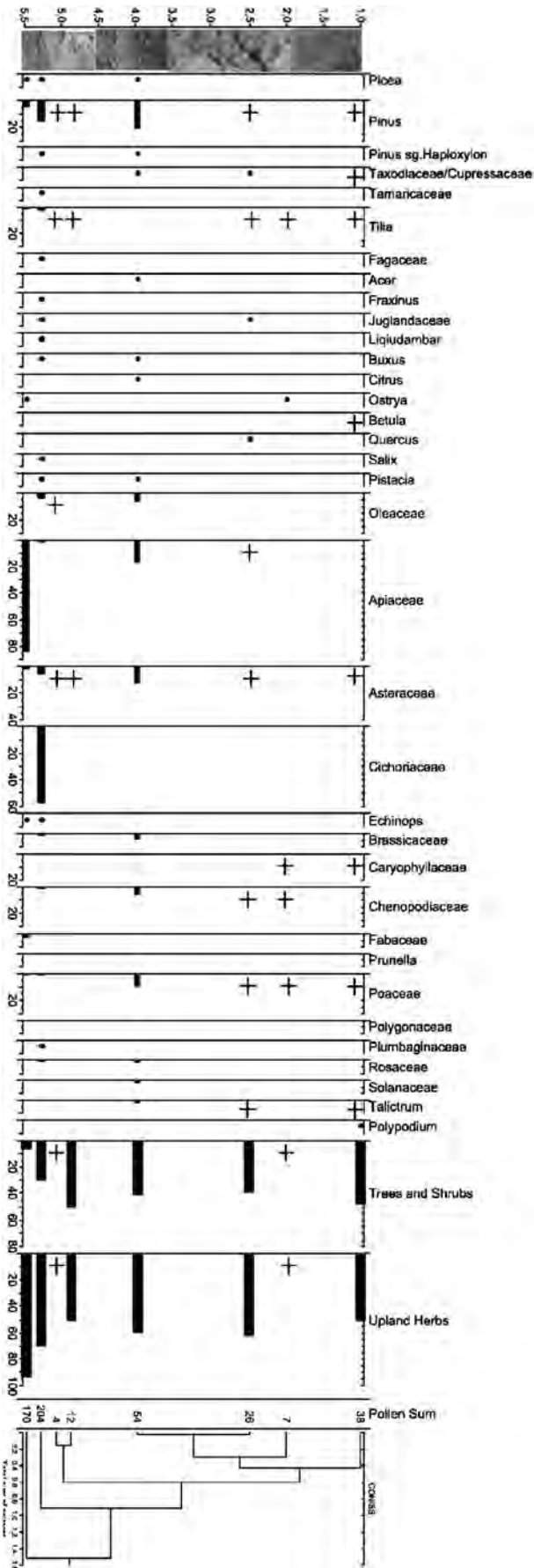
in the excavation of the upper 3 m of the Miramil quarry. The reported data date the Latamne terrace IV to  $Q_2^1$ .

Bridgland et al. (2012) re-considered the Latamne mammal fossils and concluded that they corresponded to late  $Q_1^2$  (0.9–1.2 Ma). The find of a rodent reported as *Lagurodon arankae* from Latamne (Mein and Besançon, 1993) and frequently used for indicating Early Pleistocene age of the assemblage (Bar-Yosef and Belmaker, 2011; Bridgland et al., 2012) is not diagnostic at species level but tentatively indicates a pre-Middle Pleistocene level. Two interpretations of the terrace IV age can be proposed:

First, accumulation of the terrace IV alluvium continued from the late  $Q_1^2$  to  $Q_2^1$ . The position of the fossils in the middle part of the terrace section permits this interpretation;

Second, the terrace IV alluvium was accumulated in the late  $Q_2^1$  only. In this case, there would be a gap between formation of terraces IV and III, or the Late Acheulian finds in the terrace III belong to the  $Q_2^1$ . These two variants do not correspond to the obtained data.

According to the palynological study of the Miramil quarry section (Devyatkin and Dodonov, 2000), broad-leaved pollen predominate, with *Quercus*, *Carpinus*, *Tilia Juglans*, *Ulmus* and *Corylus*.



There are also *Betula*, *Pinus*, and *Cupressus*. *Compositae* dominates in the herbaceous and shrub group. The pollen of *Gramineae*, *Artemisa*, *Chenopodiaceae*, *Ericales*, *Caryophyllaceae* and *Adonis* are rare. The assemblage indicates landscapes of grass steppes, combined with mixed forests, corresponding to wet and possibly relatively cool climate.

Finds in the terrace III alluvium were attributed to typical Late Acheulian aspect. Flat and symmetrical hand-axes were carefully fashioned by bifacial flaking. The cordiforme and ovate bifaces were made from rolled nodules or pebbles of flint and in some cases have partly preserved cortical surfaces. On the other hand, there are extremely elongated lanceolate bifaces that may derive from those of the more archaic “Latamne” type existing in the Middle Acheulian industries of the Orontes valley (Muhsen, 1985). Generally, these finds suggest an age for terrace III of late Middle Pleistocene ( $Q_2^2$ ).

Devyatkin and Dodonov (2000) reported the palynological data from terrace III. There are diverse pollen of broad-leaved (*Quercus*, *Tilia*, *Ulmus*, *Celtis*, *Carpinus*, *Corylus*, *Ostrya*, *Juglans*, and *Fagus*) and coniferous (*Pinus*, *Cedrus*, and *Cupressaceae*) trees with participation of subtropical forms: *Oleacea*, *Tamarix*, *Pistacia*, *Magnolia*, *Palmae*, *Nyssa*, and *Liquidambar*. Pollen of grasses and herbs dominate in the herbaceous and shrub group. These data indicate that the climate was wetter than at present.

The rodent teeth from the terrace II section (s 46) are dated as the Late (?) Pleistocene. Besançon et al. (1978) reported Middle and Late Paleolithic artifacts found within the Orontes terrace II alluvium ( $h = 8–15$  m) that indicated its Late Pleistocene age. According to the palynological data (Devyatkin and Dodonov, 2000), herbs and steppe grasses existed in plains and oak forests with hornbeam and linden in highlands. *Elaeagnus*, *Ilex*, and *Tamarix* occurred in valleys. The climate was pluvial. Comparison of vegetation identified in sections of the terraces IV, III and II demonstrates progressive desiccation of climate with alternation of pluvial and arid epochs, the latter being more expressive. This tendency continues in the Holocene.

## 6. The Euphrates River valley

The source of the Euphrates River is situated within the Armenian Highland. In Syria, the Euphrates valley cuts the Arabian plate (Fig. 1). From the Syrian–Turkish boundary as far as the Assad Reservoir, the river cuts the Aleppo Block, and the southward trend of the valley generally parallels the eastern margin of the block. In the Assad Reservoir area, the river turns to the ESE. It crosses the Rasafeh–El-Faid fault zone and follows the southwestern side of the Mesopotamian Basin. Farther to the SE, within Iraq, the Euphrates follows the Mesopotamian Foredeep to the Persian Gulf.

Segments of the Euphrates valley between the Assad Reservoir and the town of Abou Kamal near the Syrian–Iraq boundary are described in detail (Trifonov et al., 2012). The exposures include differentiated recent channel, flood-plain ( $h = 1–5$  m) and terraces I ( $h = 7–12$  m), II ( $h = 15–28$  m), III (undifferentiated to the SE of the town of Deir ez-Zor, where its  $h = 30–55$  m, and differentiated to sublevels III<sup>a</sup>,  $h = 30–45$  m, and III<sup>b</sup>,  $h = 45–70$  m, to the NW of Deir ez-Zor), and IV ( $h = 70–105$  m; it is identified only to the NW of Deir ez-Zor).

Neolithic industry was found on the flood-plain (Besançon and Sanlaville, 1981) and it is dated as late Pleistocene–Holocene. Terrace I is attributed to  $Q_2$ , because artifacts of the final Early and Middle Paleolithic (Levallois or “Lelallois-like” industry) are found

Fig. 9. Pollen diagram of the section (s 18) of the Orontes terrace III.

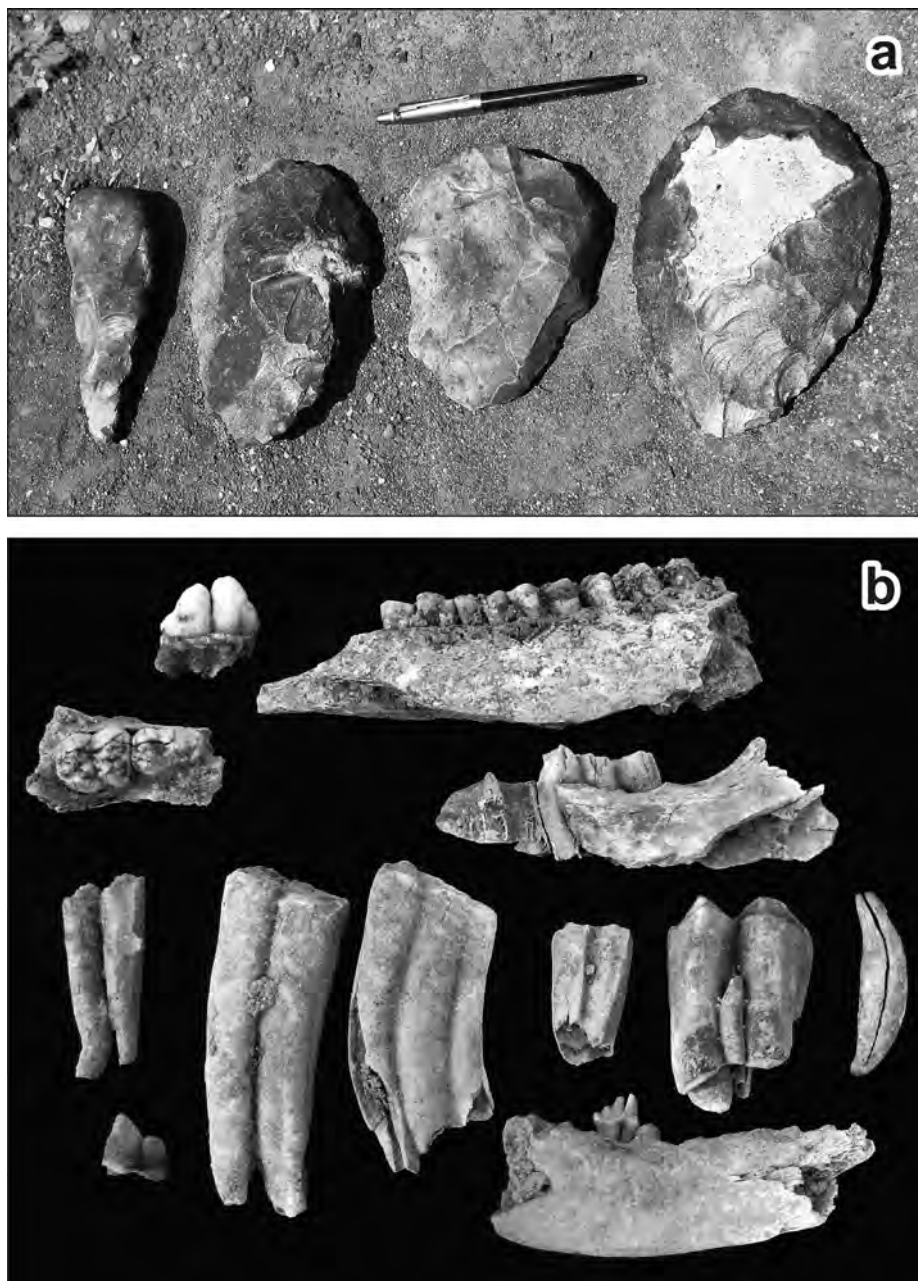


**Fig. 10.** (a) Acheulian findings in the terrace III of the Orontes River opposite the village of Khatab (s 30) and (b) fossils in the terrace IV in the village of Latamne (s 39).

in its alluvium near the village of Ayash (7 km to the NW of Deir ez-Zor) and basalts with the Ar–Ar age of  $\sim 0.4$  Ma cover the terrace alluvium (Demir et al., 2007). The archaeological finds in the terrace II alluvium, obtained in the quarry in the eastern margin of Ayash, are Acheulian. Demir et al. (2007) also reported Acheulian finds within the terrace II alluvium, while Besançon and Sanlaville (1981) attributed them to the Late Acheulian. In the same quarry, the  $\sim 3$ -m thick upper fine-grained unit of the terrace II alluvium has reverse magnetic polarity, and is covered by basalt with the K–Ar age of 0.7–0.8 Ma and normal magnetic polarity (Sharkov et al., 1998; Sharkov, 2000; Trifonov et al., 2011). By these data, the terrace II is dated as latest Early Pleistocene.

Artifacts of the Khattabian assemblage corresponding to the Oldowan culture, were found in terrace III<sup>a</sup> alluvium near the village of Kasra to the south of the Zalabiyeh–Kasra basaltic field

(Copeland, 2004; Demir et al., 2007). These finds indicate the early  $Q_1^2$  age of the terrace III<sup>a</sup>. The terrace III<sup>b</sup> is attributed to  $Q_1^1$ , because it is covered by basalt with the Ar–Ar age of  $\sim 2.12$  Ma in the southern margin of the Zalabiyeh–Kasra lava field (Demir et al., 2007). Terrace IV is dated as Late Pliocene, because the basalts of the Halabiyeh lava field with K–Ar and Ar–Ar dates of 2.7–2.8 Ma cover the terrace alluvium (Sharkov et al., 1998; Demir et al., 2007; Trifonov et al., 2011). In the Assad Reservoir area to the west of the Rasafeh–El-Faid fault zone, the terrace IV alluvium covers the unit that is mapped as Early (?) Pliocene  $N_3^a$  (Geological map, 1964).

Significant variations of height of the terraces depend on offsets on the Euphrates Fault, striking along the southwestern side of the Euphrates valley, and the transverse zones of faulting and deformation (Fig. 14). The latter are the Rasafeh–El-Faid fault zone, the Halabiyeh–Zalabiyeh fold-fault zone in the north-eastern pericline



Fig. 11. Offset and deformation of the Orontes terrace deposits in the Hama fault zone.

of the Bishri anticline of the Palmyrides, and probably the Abou Kamal fold-fault zone, bordering the Euphrates Fault to the SE (Trifonov et al., 2012).

Vertical offsets on the Euphrates Fault are registered by elevation of the terraces in the southwestern side of the valley above the same terraces in the northeastern side. In the Assad Reservoir area, the offset of terrace IV does not exceed ~10 m. The fault thus attenuates in the Aleppo Block. Eastwards, near the Rasafeh–El-Faid zone, the offset of terrace IV reaches 20–30 m. The difference of altitudes of the terrace III is 12–20 m on the different sides of the valley, and terrace III<sup>b</sup> is offset to a greater magnitude (15–25 m) than the terrace III<sup>a</sup> (12–15 m) to the east of the town of Ar Raqqa

and in the Halabiyeh–Zalabiyeh area. Terrace II is offset to 2–6 m. An analogous difference of height of terrace I was found only to the SE of Deir ez-Zor, although a small offset was registered also near the town of Ar Raqqa (Trifonov et al., 2012). These data show that the Euphrates fault developed during the Pliocene and Quaternary, and movements on the fault were essentially decelerated to the NW of Deir ez-Zor after the Middle Pleistocene.

Movements on the transverse zones of faulting and deformation are expressed by uplift and splitting of the terraces III and IV in the eastern side of the Rasafeh–El-Faid fault zone and in the Halabiyeh–Zalabiyeh area (Trifonov et al., 2012). The terraces of the latter area are also offset on small transverse faults, feathering out

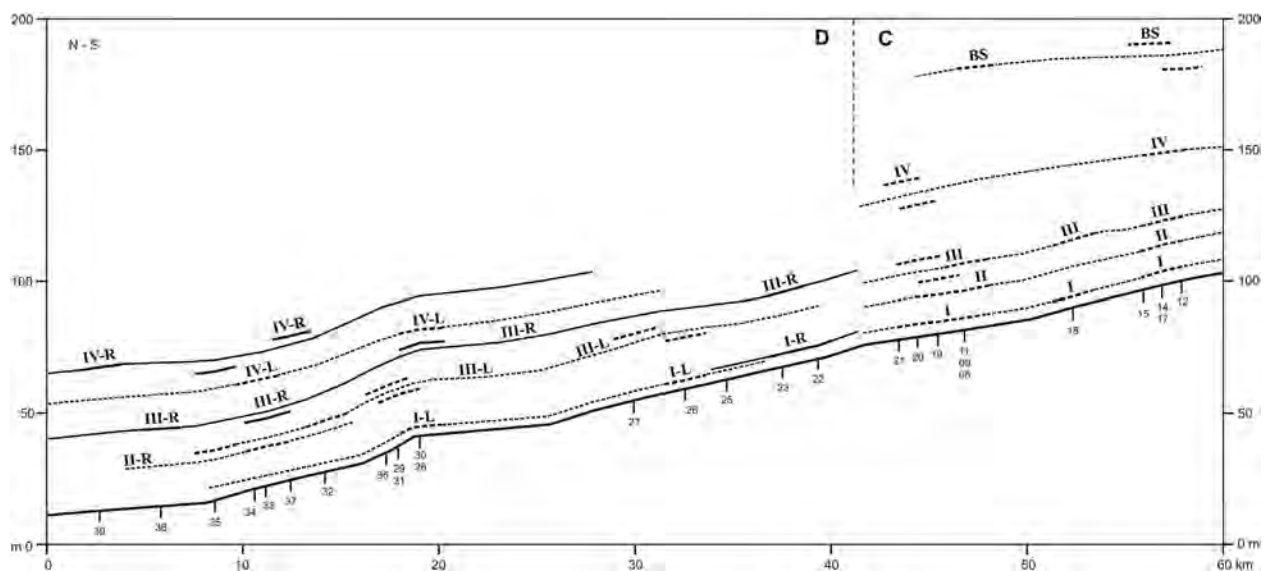
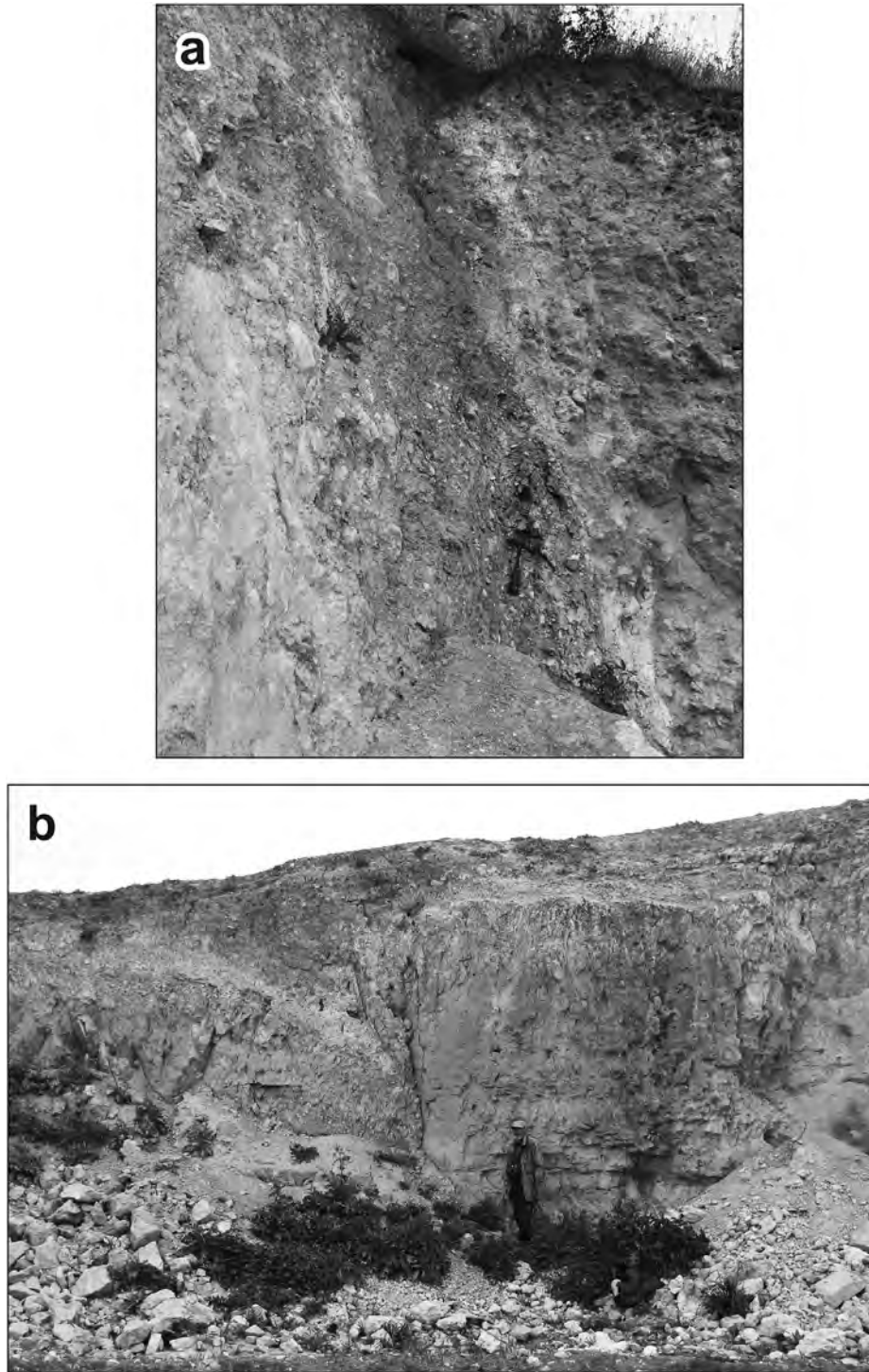


Fig. 12. Geomorphological profile along segment D of the Orontes River valley, based on combined evidence; “R” is the NE side of the Hama fault and “L” is the SW side.



**Fig. 13.** Offsets of the Orontes terraces on active faults: a, the village of Chizar (s 40) and b, to the north-west of it (s 42).

to the north (Abou Romieh, 2009). The recent activity of the Euphrates Fault as well as activity of some segments of the Rasafeh–El-Faid zone are confirmed by the records of historical earthquakes: 160 AD (N34.7° and E40.7°;  $M_s = 6.0$ ), 800–802 (N35.7° and E38.7°;  $M_s = 6.1$ ), and 1149 (N35.9° and E39.0°;  $M_s = 6.6$ ) (Kondorskaya and Shebalin, 1982; Guidoboni et al., 1994; Kondorskaya and Ulomov, 1999; Sbeinati et al., 2005).

In the Aleppo Block near the Syrian–Turkish boundary, the oldest Euphrates alluvium ( $h = 80–90$  m to 120 m) is found in the

northeastern side of the Euphrates valley. This level is composed of the tens of meters thick  $N_2^3$  unit of the Euphrates pebbles and sands (Geological map, 1964). Near the town of Jrablus, four terraces are incised into the  $N_2^3$  surface: QfI ( $h \approx 8$  m), QfII ( $h = 20–30$  m), QfIII ( $h = 40–45$  m), and QfIV ( $h \approx 70$  m) (Copeland, 2004; Sanlaville, 2004). These authors reported archaeological finds within the terrace alluvium: early Paleolithic industry without hand-axes in terrace QfIV; Acheulian hand-axes in terrace QfIII; and Levallois-like type in terrace QfII. Demir et al. (2008) supposed that the

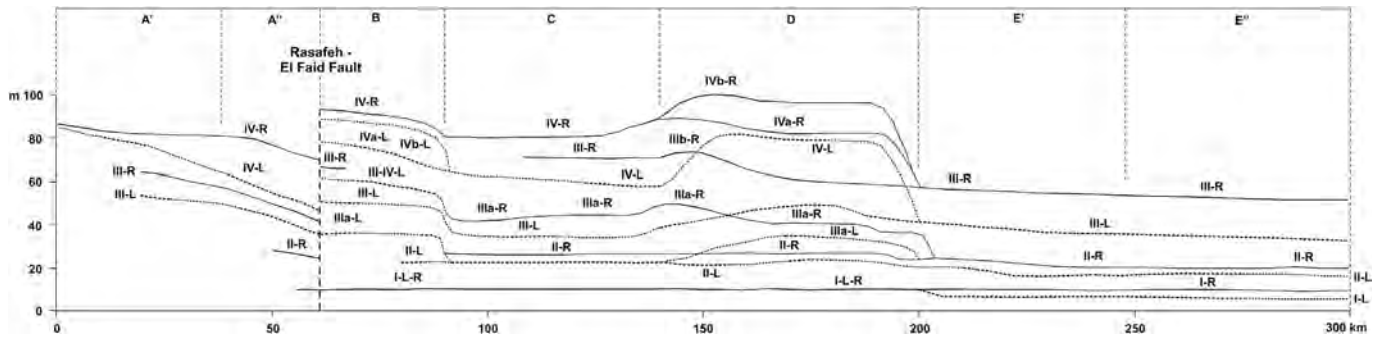


**Fig. 14.** Geomorphological profile along the Euphrates valley downstream the Assad Reservoir, based on combined evidence; “r” is the right bank and “l” is the left bank of the valley (Trifonov et al., 2012).

terrace ( $h = 40–45$  m) corresponds to MIS14 or MIS16 (~540–640 ka).

Demir et al. (2008) studied the Euphrates terraces in the Biresik segment of the river to the north of the Syrian–Turkish boundary. The İt Dağı gravel composes the highest terrace ( $h \approx 130$  m). The lower terraces are represented by the surface of the Arslanatağı Sirti upper gravel ( $h \approx 108$  m), levels of  $\sim 87$  m and  $\sim 77$  m, and the surface of the Bayındır gravel ( $h = 55–60$  m,  $M \approx 45$  m). The terraces  $\sim 45$ ,  $\sim 35$ ,  $\sim 21$ ,  $\sim 8$  and  $\sim 2$  m are incised into the surface of the Bayındır gravel. Acheulian hand-axes are reported from the lower part of the Bayındır section, and primitive early Paleolithic artifacts, identified with the Oldowan culture are reported from the Tilmağara gravel ( $h$  is up to 80 m).

**7. Chrono-stratigraphic correlation of the terraces**

The data allow the possibility of correlating the terraces of different segments of the Euphrates (Table 3). The El-Kabir and Orontes terraces, dated to early Middle Pleistocene to Holocene, are also satisfactorily intercorrelated. The lower Euphrates terraces upstream of the Assad Reservoir probably correspond to them. However, only the Euphrates terrace I corresponds to this terrace sequence downstream, between the Assad Reservoir and Abou-Kamal. The higher Euphrates terraces are older. They were formed in Pliocene and Early Pleistocene. The recent Orontes and El-Kabir valleys only began to develop in the late Early Pleistocene.

The age and, correspondingly, correlation of the Syrian fluvial terraces can be defined more accurately by attribution of the terrace deposits to the MIS. Bridgland and Westaway (2008) carried out a worldwide comparison of fluvial terraces and showed that their formation was a response to climatic fluctuation, switching to the 100 ka Milankovitch cycle since the beginning of Middle Pleistocene. Incision can accelerate both during the cold-to-warm or warm-to-cold transition. The majority of researchers of the Syrian large river terraces assume the second scenario (Besançon et al., 1978; Copeland and Hours, 1993; Bridgland et al., 2012). However, sediments of the Tyrrhenian marine terrace in the Mediterranean coast of Syria were dated by the  $^{230}\text{Th}/\text{U}$  method to 128.5–83.4 ka, i.e., the Eemian interglacial, MIS5e (Dodonov et al., 2008). Perhaps, the higher marine terraces were formed also during interglacial transgressions. We observed intercalation of the marine and alluvial MIS1 sediments in the recent beach near the El-Kabir mouth as well as in the terrace II sections near the mouth of the Snoubur River and some smaller rivers of the coast. In the lower part of the El-Kabir valley, we registered a transition from the marine terrace II (Tyrrhenian) to the terrace II composed of alluvium. All these data demonstrate synchronicity of the marine and river terrace sediments.

Palynological data of A.N. Simakova (Dodonov et al., 2008) on the Arab el Mulk Tyrrhenian marine terrace section indicate relatively arid conditions of accumulation of its lowest part (interval of 2.5–3.0 m) and higher humidity during accumulation of the major part of the section (interval of 2.5–0.8 m). To interpret these data, it

**Table 3**  
Correlation of terraces of the large Syrian rivers and height of the terraces, m.

Age of alluvium/age of following incision;	MIS of incision and sedimentation of alluvium/MIS of following incision	Coastal Range, Nahr El-Kabir		Aleppo Block, Orontes	Aleppo Block, Euphrates, Birecik → Jرابلس <sup>a</sup>	Mesopotamian Foredeep, Euphrates downstream the Assad Reservoir <sup>b</sup>
		NW	SE			
$N_2$ ; >3 Ma		Sea gulf		Low highland, basins in the NW (& the S in $N_2$ )	VII: 130 → 120	Basin, existing in the SW till $Q_1^1$
$N_2^2$ ; >2.7 Ma/<2.7 Ma					VI: 108 → ?	IV: 70–105
$Q_1^1$ ; >2.1 Ma/<2.1 Ma					V: ~80 → 70	III <sup>b</sup> : 45–70
Early $Q_1^2$ ; ~1900–1550 ka/1550–1400 ka				$Q_1$ : 80–100		III <sup>a</sup> : 30–45
Late $Q_1^2$ ~1400–800 ka/~800 ka	MIS46–21/MIS20	V: ~130		IV: 43–60	IV: 56 → 45	II: 15–25
$Q_1^3$ ~800–500 ka/~500 ka	MIS20–15/MIS14	IV: 112–120	IV: 95–108		III: 40 → 30	I: ~10
$Q_2^2$ ~400–280 ka/~270 ka	MIS12–9/MIS8	III <sup>b</sup> : 90–100	III <sup>b</sup> : 71–73	III: 20–35	II: ~20	
		III <sup>a</sup> : 70–81	III <sup>a</sup> : 47–59			
$Q_3^1$ ~90–130 ka/80 ka	MIS6–5/MIS4	II <sup>b</sup> : 41	II <sup>b</sup> : 24–38	II: 7–15	I: ~8	High flood-plain: up to 5
		II <sup>a</sup> : 15–22	II <sup>a</sup> : 7–17			
$Q_3^2$ – $Q_4$ , 50–10 ka/26–0 ka	MIS4–1/MIS2–0	I/high flood-plain: 4–6 ( $Q_4$ )		I/high flood-plain: 2–4	0: ~2	

<sup>a</sup> The Birecik segment, southeast Turkey, and the Jرابلس segment, north Syria, after (Sanlaville, 2004; Demir et al., 2008).

<sup>b</sup> After (Demir et al., 2007; Trifonov et al., 2012).

is necessary to take into account that the Arab el Mulk section represents the beginning of the Tyrrhenian transgression (the  $^{230}\text{Th}/\text{U}$  date is  $128.5 \pm 10.4$  ka), i.e., the section shows increasing precipitation at the beginning of the interglacial. Pluvial conditions are characteristic for the main parts of the sections of alluvial deposits of the El-Kabir terrace IV and the Orontes terraces IV (Latamne), III (s 18) and II. A decrease of precipitation was registered in the upper parts of the sections of the El-Kabir terrace IV Jindiriyeh and the Orontes terrace III (s 18). According to the palynological study of the Palestine archaeological sections (Leroi-Gourhan and Darmon, 1987), the last glacial epoch (MIS2) was characterized by arid conditions with a trend to a more pluvial phase at  $\sim 14$ – $15$  ka. Precipitation reached maximum at the beginning of Holocene ( $Q_4$ ). Correlation of the cited data with paleoclimatic indicators in the adjacent regions of Near and Middle East and Northern Africa (Trifonov and Karakhanian, 2004) shows that the humidification began in these regions at  $\sim 14$ – $10$  ka, showed some fluctuation, and proceeded differently in different regions. It reached its maximum generally in the early Atlantic. Later, desiccation with relatively pluvial episodes took place (Issar and Zohar, 2007).

The formation of alluvial terraces is caused by variations of incision rates in river valleys. The latter can depend on either tectonic processes and/or climatic changes. First, the world sea level and, correspondingly, base level of erosion of rivers change and, second, erosion increases with rising precipitation. The base level was similar to the recent one or exceeded it by up to  $\sim 5$  m during the Tyrrhenian marine transgression (the  $Q_3$  interglacial). It was likely approximately the same during accumulation of sediments of the earlier marine terraces of  $Q_2$  and late  $Q_1$ . The level was  $\sim 100$  m lower during the glacial epochs. A fall of the base level during glacial epochs allowed incision of rivers. It occurred only partly during glacial epochs because of the arid climate and accelerated with a rise of precipitation during deglaciation and particularly at the beginning of interglacials when the main mass of alluvium, relatively coarse because of intensive erosion, was accumulated. The upper fine-grained part of the alluvium was accumulated in the later interglacial that was characterized by desiccation and decreasing erosion. A fall of sea level during the next glacial was a precondition for the following incision and the cycle repeated. The cycle from incision starts at the glacial epoch and continues during the interglacial, i.e., it mostly spans the “odd” MIS stages.

The factors under discussion acted differently in the different river valleys of Syria. The Levant coast of the Mediterranean is steep. The glacial/interglacial variation of sea level directly caused the incision and initiated the cycle of terrace formation in the inflowing rivers. This is characteristic for the El-Kabir and Orontes. The situation was different in the Euphrates valley. Because of the very gentle longitudinal slope of the Mesopotamian Basin, fall of the base level in the glacial epochs resulted in significant retreat of the Persian Gulf water level, lengthening the longitudinal profile of the river. Finally, the gradient of the longitudinal slope almost did not affect the intensity of the incision. Climatic changes acted only to change the intensity of erosion because of variations of precipitation. If the rate of uplift was relatively high (Birecik and Jرابلس areas), this resulted in formation of the terrace stair, analogous to the stairs in the Orontes and El-Kabir valleys. If the rate was small, effects of the climatic variations decreased. As a result, the Euphrates terraces I and II between the Assad Reservoir and Abou Kamal formed over a long time, corresponding to several MIS stages.

Besançon and Sanlaville (1981) reported a finding of the Euphrates alluvium in the boreholes in the town of Ar-Raqqa at 35 m depth and in the village of Tabni to the SE of the Halabiyeh lava field 27 m below the recent Euphrates level. Perhaps, the

$\sim 45$  m thick Bayindir gravel with the Acheulian artifacts, which occupies the interval between 10–11 m and  $\sim 56$  m above the Euphrates in the Birecik segment of the valley, is an analogous feature (Demir et al., 2008). Besançon and Sanlaville (1981) explained these features by overdeepening of the valley before terrace II formation. However, the presence of basement in the adjacent sections of terrace II does not confirm overdeepening. Sinkholes up to several meters wide and 3 m deep in the  $N_2$  clay, marl and gypsum, infilled with Euphrates gravel, underlie the terrace II alluvium near the villages of Jdetdet Mkhét and Hamret Nasser (Trifonov, 2012). The sinkholes were caused by leaching of gypsum and eluviation of clay of the  $N_2$  bedrock by ground waters. Similar but larger structures are seen in the east of the Abdel Aziz anticline in the Tortonian, composed of clays, silts, marls, and gypsum. The largest of such depressions,  $200 \times 400$  m wide and up to 50 m deep, is situated in the site N36.46026° and E40.65510°. The boreholes mentioned by Besançon and Sanlaville (1981) are also situated within the Tortonian. The local subsidence of the valley bottom was very probable before the II terrace formation, and the Euphrates fault activity could have accelerated the ground water flow.

## 8. Quaternary uplift in Syria by the data on fluvial terraces

The river valleys belong to different tectonic provinces of Syria. Nahr El-Kabir is situated in the anticlinal Coastal Range, which spread to the north in the Late Pliocene and Quaternary and occupied the on-shore part of the El-Kabir Basin and the Bassith Block. The studied segments of the Orontes flow through the platform Aleppo Block that is weakly elevated relative to the main part of the Arabian Plate. The Syrian segment of the Euphrates upstream of the Assad Reservoir and the adjacent Turkish Birecik segment are situated in the eastern Aleppo Block. Between the mouths of the Rasafeh and El-Faid tributaries and the town of Abou Kamal, the Euphrates flows along the south-western side of the Mesopotamian Foredeep.

Stairs of the river terraces indicate tectonic uplift of the region. Although the magnitude of incision, causing isolating of a terrace and accumulation of younger alluvium within a valley does not correspond exactly to magnitude of the uplift, the difference of the terrace height within a single valley and between valleys reflects the tendency of vertical movements. Such differences indicate the Quaternary offsets on faults. These are the Lattaqieh Fault in the El-Kabir valley (Table 1; Figs. 2, 5 and 6), the Hama Fault and the transverse faults in the Orontes valley (Table 2; Figs. 5c, 7 and 12), and the Euphrates Fault and the transverse zones of faulting and deformation in the Euphrates valley (Figs. 1 and 14). Ignoring this local deformation indicates the difference of the incision values in the different tectonic provinces (Table 3).

The El-Kabir terraces characterizing the Coastal Range are the most uplifted. The Orontes terraces in the Aleppo Block are lower. The terraces are particularly low in the south of the block where the Orontes cuts the Homs Basin. To the north, the height of the terraces increases, but even there, they are approximately twice as low as the correlated El-Kabir terraces. The Euphrates terraces upstream of the Assad Reservoir are a little lower than the comparable Orontes terraces and 2.5 times lower than the El-Kabir terraces. The correlated Euphrates terraces downstream of the Assad Reservoir characterizing the southwestern side of the Mesopotamian Foredeep are 2–3 times lower than the terraces of the upstream Euphrates and Orontes.

We calculated average rates of the incision in different valleys during different epochs, dividing the height of the higher terrace above the lower one by the time interval between the beginning of the incision into their alluvium and using estimates of their ages by

correlation with the MIS scale. These estimates are tentative because of inaccuracy of the terrace dating and express only a general tendency. Application of this technique to offsets of the terraces on the Lattaqieh Fault showed that the fault movements accelerated from ~70 mm/ky during ~270–80 ka to ~100 mm/ky during ~80–10 ka (see Table 1). The rate of motion on the Hama Fault is estimated as 16–36 mm/ky. The segments of the Euphrates Fault to the SE of the Rasafeh–El-Faid fault zone demonstrate that the displacements were absent or small since the beginning of incision into terrace IV alluvium (~2.6–2.7 Ma) until the beginning of incision into terrace III<sup>b</sup> alluvium (~2.1 Ma). The rate was 10–

incision during the entire interval, the comparison of the rates demonstrates the main regularity. The rates of incision are ~220–280 mm/ky in the Coastal Range (the El-Kabir River) and ~80–130 mm/ky in the Aleppo Block (the Orontes River and the Biresik–Jrablus segments of the Euphrates). The rates decrease to ~25–30 mm/ky in the south-western side of the Mesopotamian Foredeep (the Euphrates River downstream the Assad Reservoir). These rates correspond approximately to the intensity of the Middle and Late Quaternary uplift in different provinces of Syria and give the quantitative estimates of tendencies that were outlined in the Pliocene and Early Pleistocene.

**Table 4**  
Rates of incision of river valleys in different tectonic provinces of Syria, mm/ky.

Province, river, terrace				Beginning of incision into the valley (formation of the terrace), ka													
Province	River	Terrace	h, m	Δh, m	3200	2700	2100	1500	800	500	400	270	140	80	14		
Coastal Range	Nahr El-Kabir	V	~130	~14					~50								
		IV	102–116	~26						~110							
		III <sup>b</sup>	72–95	~48									~250				
		II <sup>b</sup>	31–41	~31											~470		
		I	~5	~5												~360	
Homs Basin	Orontes	III	~20	~11.3								~60			~90		
		II	~8.7	~6												~190	
		I	~2.7	~2.7													
Aleppo Block	Euphrates, Birecik	V	80–100	29–49				29–49									
		IV	~51	~25						~110 <sup>a</sup>							
		III	~26	~11									~60				
		II	~15	~11.6											~180		
		I	~3.4	~3.4												~240	
		VII	132	24	~22												
		VI	108	~28				~47									
		V	~80	~24				~34									
		IV	56	~16						~53							
		III	~40	~19							~100						
		II	21	13								~50					
		I	8	6										~48			
		0	2	2												~190	
		Euphrates, Jrablus	V	~100	~30	~18											
			IV	~70	~28				~28								
III	40–45		~17							~170							
II	~25		~17								~65						
I	8		6										~48				
0	2		2												~190		
V	~100		~30	~18													
Mesopotamian Foredeep	Euphrates, Raqqa – Abou Kamal	IV	~88	~30		~50											
		III <sup>b</sup>	~58	~20				~33									
		III <sup>a</sup>	~38	~16				~23									
		II	~22	~12						~30							
		I	~10	~7								~27					
		0	~3	~3										~21			
		0	~3	~3											~21		

<sup>a</sup> If formation of the terrace IV finished in the Orontes at the Late Calabrian, the rate of incision reduces 1.5–2 times.

11 mm/ky from ~2.1 Ma till ~0.4 Ma, increasing to 12–15 mm/ky in the Halabiyeh–Zalabiyeh zone and decreasing up to 8–10 mm/ky to the SE. After ~0.4 Ma, the rate was the same to the SE of the Halabiyeh–Zalabiyeh zone, but sharply decreased in this zone and to the NW (Trifonov et al., 2012).

Application of the same technique to comparison of uplifts in the different tectonic provinces gives the following results (Table 4). In the valleys except the Euphrates downstream of the Assad Reservoir, the rates of incision were small at the early stage of the valley formation and increased later. Comparison of the valleys is possible only for Middle and Late Pleistocene, because the earlier incision is absent in the El-Kabir and Orontes. Some temporal intervals demonstrate the abnormally high rates of incision relative to the other temporal intervals in the same valley, perhaps, because of incorrect correlation of the terraces with the MIS scale. After smoothing these anomalies by calculation of the average rates of

## 9. Conclusions

Using paleontological, archaeological, paleomagnetic and radio-isotopic methods, the ages of the El Kabir and Orontes river terraces was determined and correlated with the Euphrates terraces. Evidence of synchronism of the El-Kabir alluvial terraces and the marine terraces in the Mediterranean coast of Syria as well as palynological correlation of the marine and river terraces allowed correlation of stages of the river terraces formation with climatic changes and MIS. River incision resulting in isolation of the former valley bottom as a terrace began at a glacial epoch and developed most intensively during deglaciation and early interglacial. Accumulation of the main part of the coarse alluvium occurred at the same pluvial stage. A finer-grained upper part of the alluvium is attributed to a more arid late interglacial. Average rates of incision in the valleys during different time intervals were estimated

tentatively by using relative heights of the terraces and the defined ages of stages of terrace formation. These rates correspond approximately to the rates of Quaternary uplift in different tectonic provinces of Syria and vertical movements on the Lattaqieh fault in the El-Kabir valley, the Hama fault in the Orontes valley and the Euphrates fault in the Euphrates valley. The rates of incision were usually small in the earlier stages of the terrace formation and increased later. Comparison of average rates of incision in different valleys during the Middle and Late Pleistocene demonstrates that the rates are: ~220–280 mm/ky in the El-Kabir valley (the Coastal Range), ~80–130 mm/ky in the Orontes valley and the Euphrates valley upstream of the Assad Reservoir (the Aleppo Block), and ~25–30 mm/ky in the Euphrates downstream of the Assad Reservoir (southwestern side of the Mesopotamian Foredeep).

## Acknowledgements

V.G. Trifonov, D.M. Bachmanov, A.N. Simakova, Ya.I. Trikhunkov, O.Ali and A.M. Al-Kafri carried out the geological and geomorphological studies. A.S. Tesakov analysed the paleontological collection and E.V. Belyaeva and V.P. Lyubin studied the archaeological finds. A.N. Simakova carried out the palynological studies and R.V. Veselovsky conducted the paleomagnetic study of the Euphrates terrace II alluvium. The studies were supported by the Program 6 “Dynamics of the continental lithosphere: Geological and geophysical modelling” of the Department of Geosciences of the RAS, the Grants 11-05-00628-a and 13-06-12016 OFI\_m of the Russian Foundation for Basic Research, and the Project “Geodynamics of Syria” of the GORS, Syria.

## References

- Abou Romieh, M., Westaway, R., Daoud, M., Radwan, Y., Yassminh, R., Khalil, A., al-Ashkar, A., Loughlin, S., Arrell, K., Bridgland, D., 2009. Active crustal shortening in SE Syria revealed by deformed terraces of the River Euphrates. *Terra Nova* 21 (6), 427–437.
- Barazangi, M., Seber, D., Chaimov, T., Best, J., Litak, R.D., Sawaf, T., 1993. Tectonic evolution of the northern Arabian plate in western Syria. In: Boschi, E., Mantovani, E., Morelli, A. (Eds.), *Recent Evolution and Seismicity of the Mediterranean Region*. Kluwer Academic Publishers, Dordrecht, pp. 117–140.
- Bar-Yosef, O., Belmaker, M., 2011. Early and Middle Pleistocene faunal and hominins dispersals through Southwestern Asia. *Quaternary Science Reviews* 30, 1318–1337.
- Besançon, J., 1981a. Stratigraphie et chronologie du Quaternaire continental du Proche Orient. *Colloques Internationaux du C.N.R.S.* 598, 33–53.
- Besançon, J., 1981b. Chronologie du Pleistocene au Levant. *Colloques Internationaux du C.N.R.S.* 598, 145–153.
- Besançon, J., Copeland, L., Hours, F., Sanlaville, P., 1977. Sur le Quaternaire de la region de Lattaquie (Syrie). *Comptes rendues academie des sciences* 284, 16–32.
- Besançon, J., Copeland, L., Hours, F., Sanlaville, P., 1978. The Palaeolithic sequence in Quaternary formations of the Orontes river valley, Northern Syria: a preliminary report. *Bulletin, Institute of Archaeology, University of London* 15, 149–170.
- Besançon, J., Sanlaville, P., 1981. Aperçu geomorphologique sur la vallee de l'Euphrate Syrien. *Paleorient* 7 (2), 5–18.
- Besançon, J., Sanlaville, P., 1993. Remarques sur la geomorphologie du Ghab (Syrie). Chapitre II. Paleolithique de la vallee moyenne de l'Orontes (Syrie). *British Archaeological Reports International Series* 587, 41–56.
- Bridgland, D.R., Philip, G., Westaway, R., White, M., 2003. A long Quaternary terrace sequence in the Orontes River valley, Syria: a record of uplift and of human occupation. *Current Science* 84 (8), 1080–1089.
- Bridgland, D.R., Westaway, R., 2008. Clinatically controlled river terrace staircases: a worldwide Quaternary phenomenon. *Geomorphology* 98, 285–315.
- Bridgland, D.R., Westaway, R., Daoud, M., Yassminh, R., Abou Romieh, M., 2008. River terraces of the Nahr el Kebir, NW Syria, and their Palaeolithic record. *CBRL Bulletin* 3, 36–41.
- Bridgland, D.R., Westaway, R., Abou Romieh, M., Candy, I., Daoud, M., Demir, T., Caliaatsos, N., Schreve, D.C., Seyrek, A., Shaw, A.D., White, T.S., Whittaken, J., 2012. The River Orontes in Syria and Turkey: downstream variation of fluvial archives in different crustal blocks. *Geomorphology* 165–166, 25–49.
- Clark, J.D., 1967. The Middle Acheulian occupation site at Latamne, Northern Syria. *Quaternaria* 9, 1–68.
- Clark, J.D., 1968. The Middle Acheulian occupation site at Latamne, Northern Syria: further excavation. *Quaternaria* 10, 1–76.
- Copeland, L., 1981. Chronology and distribution of the Middle Paleolithic, as known in 1980, in Lebanon and Syria. *Colloques Internationaux du C.N.R.S.* 598, 239–263.
- Copeland, L., 2004. The paleolithic of the Euphrates Valley in Syria. *British Archaeological Reports International Series* 1263, 19–114.
- Copeland, L., Hours, F., 1978. La séquence Acheuléenne du Nahr el Kebir région septentrionale du littoral Syrien. *Paleorient* 4, 5–29.
- Copeland, L., Hours, F., 1993. The Middle Orontes paleolithic flint industries. *British Archaeological Reports International Series* 587, 63–144.
- Demir, T., Westaway, R., Bridgland, D., Pringle, M., Yurtmen, S., Beck, A., Rowbotham, G., 2007. Ar-Ar dating of Late Cenozoic basaltic volcanism in northern Syria: Implications for the history of incision by the River Euphrates and uplift of the northern Arabian Platform. *Tectonics* 26. <http://dx.doi.org/10.1029/2006TC001959>. TC 3012.
- Demir, T., Seyrek, A., Westaway, R., Bridgland, D., Beck, A., 2008. Late Cenozoic surface uplift revealed by incision by the River Euphrates at Birecik, southeast Turkey. *Quaternary International* 186, 132–163.
- Devyatkin, E.V., Dodonov, A.E., Gablina, S.S., Golovina, L.A., Kurenkova, V.G., Simakova, A.N., Trubikhin, V.M., Yasamanov, N.A., Khatib, K., Nseir, H., 1996. Upper Pliocene–Lower Pleistocene marine deposits of Western Syria: Stratigraphy and paleogeography. *Stratigraphy and Geological Correlation* 4 (1), 67–77.
- Devyatkin, E.V., Dodonov, A.E., 2000. Stratigraphy of the Neogene and Quaternary deposits. In: Leonov, Yu.G. (Ed.), *Outline of Geology of Syria*. Nauka, Moscow, pp. 129–176 (in Russian).
- Dodonov, A.E., Devyatkin, E.V., Ranov, V.A., Khatib, K., Nseir, H., 1993. The Latamne formation in the Orontes River Valley. *British Archaeological Reports International Series* 587, 189–194.
- Dodonov, A.E., Trifonov, V.G., Ivanova, T.P., Kuznetsov, V.Yu., Maksimov, F.E., Bachmanov, D.M., Sadchikova, T.A., Simakova, A.N., Minini, H., Al-Kafri, A.-M., Ali, O., 2008. Late Quaternary marine terraces in the Mediterranean coastal area of Syria: geochronology and neotectonics. *Quaternary International* 190, 158–170.
- Geological Map of Syria, 1964. Scales 1:200 000 and 1:500 000. In: Ponicarov, V. (Ed.), *Technoexport, Moscow; Ministry of Industry of the S.A.R., Damascus*.
- Gomez, F., Khawlie, M., Tabet, C., Darkal, A.N., Khair, K., Barazangi, M., 2006. Late Cenozoic uplift along the northern Dead Sea transform in Lebanon and Syria. *Earth and Planetary Sciences Letters* 241, 913–931.
- Guérin, C., Eisenmann, V., Faure, M., 1993. Les grands mammifères du gisement Pléistocène Moyen de Latamné (vallée de l'Oronte, Syrie). *British Archaeological Reports International Series* 587, 169–178.
- Guidoboni, E., Comastri, A., Traina, G., 1994. Catalogue of Ancient Earthquakes in the Mediterranean Area up to the 10th Century. *Istituto Nazionale di Geofisica, Rome*, p. 504.
- Hooijer, D.A., 1962. Middle Pleistocene mammals from Latamne, Orontes valley, Syria. *Annales Archaeologiques de Syrie (Damascus)* 11, 117–132.
- Hours, F., 1981. Le Paleolithique inferieur de la Syrie et du Liban. Le point de la question en 1980. In: Sanlaville, P., Cauvin, J. (Eds.), *Prehistoire du Levant. Maison de l'Orient, Lyon*, pp. 165–184.
- Ilhan, E., 1974. Eastern Turkey. In: Spencer, A.M. (Ed.), *Mesozoic–Cenozoic Orogenic Belts*, vol. 1. Scottish Academic Press, Edinburgh.
- Issar, A.S., Zohar, M., 2007. *Climate Change – Environment and History of the Near East*, second ed. Springer, Berlin.
- Kondorskaya, N.V., Shebalin, N.V. (Eds.), 1982. *New Catalog of Strong Earthquakes in the USSR from Ancient Times Through 1977*. World Data Center A for Solid Earth Geophysics. NOAA, Boulder, CO.
- Kondorskaya, N.V., Ulomov, V.I. (Eds.), 1999. *Special Catalogue of Earthquakes of the Northern Eurasia (SECNE), Global Seismic Hazard Assessment Program, Zurich, Switzerland*. <http://www.seismo.ethz.ch/gshap/neurasia/nordasiacat.txt>.
- Leroi-Gourhan, A., Darmon, F., 1987. Analyses palynologiques de sites archéologiques du Pleistocene final dans la vallee du Jourdain. *Israeli Journal of Earth Sciences* 36, 65–72.
- Martini, E., 1971. In: Farinacci, A. (Ed.), *Standard Tertiary and Quaternary Calcareous Nannoplankton Zonation, Proceeding of the Second Planktonic Conference, Roma, 1970*, vol. 2. Tecnoscienza, Roma, pp. 739–785.
- Mein, P., Besançon, J., 1993. Micromammifères du Pléistocène Moyen de Latamné. In: Sanlaville, P., Besançon, J., Copeland, L., Muhesen, S. (Eds.), *Le Paléolithique de la vallée moyenne de l'Oronte (Syrie): Peuplement et environnement*, *British Archaeological Reports, International Series*, vol. 587, pp. 179–182.
- Muhesen, S., 1985. L'Acheuleen Recent Evolue de Syrie. *British Archaeological Reports International Series* 248, 1–189.
- Ponicarov, V.P., Kazmin, V.G., Mikhailov, I.A., Razvalyayev, A.V., Krashennnikov, V.A., Kozlov, V.V., Souliidi-Kondratyev, E.D., Mikhailov, K.Ya., Kulakov, V.V., Faradjev, V.A., Mirzayev, K.M., 1967. *Geological Map of Syria, Scale 1:500,000*. Explanatory Notes, Part I. Ministry of Industry, Damascus, p. 230.
- Rio, D., Sprovieri, R., Thunell, R., 1991. Pliocene–Lower Pleistocene chronostratigraphy: a re-evaluation of Mediterranean type sections. *Geological Society of America Bulletin* 103, 1049–1058.
- Robertson, A.H.F., 2000. Mesozoic–Tertiary tectonic–sedimentary evolution of south Tethyan oceanic basin and its margins in southern Turkey. In: *Tectonics and Magmatism in Turkey and the Surrounding Area*. Geological Society of London Special Publications, vol. 173, pp. 97–138.
- Robertson, A., Unlüğenç, Ü.C., Inan, N., Taşli, K., 2004. The Misis–Andirin Complex: a Mid-Tertiary melange related to late-stage subduction of the Southern Neotethys in S. Turkey. *Journal of Asian Earth Sciences* 22 (5), 413–453.

- Rukieh, M., Trifonov, V.G., Dodonov, A.E., Minini, H., Ammar, O., Ivanova, T.P., Zaza, T., Yusef, A., Al-Shara, M., Jobaili, Y., 2005. Neotectonic map of Syria and some aspects of Late Cenozoic evolution of the north-western boundary zone of the Arabian plate. *Journal of Geodynamics* 40, 235–256.
- Sanlaville, P. (Ed.), 1979. Quaternaire et préhistoire du Nahr el Kabir septentrional: les debuts de l'occupation humaine dans la Syrie du Nord et au Levant. Coll. Maison Orient. C.N.R.S.9, Lyon, p. 162.
- Sanlaville, P., 1981. Stratigraphie et chronologie du Quaternaire marin du Levant, vol. 598. *Colloques Internationaux du C.N.R.S.*, pp. 21–31.
- Sanlaville, P., 2004. Les terraces Pléistocènes de la vallée de l'Euphrate en Syrie et dans l'extrême sud de la Turquie. In: *British Archaeological Reports, International Series*, vol. 1263, pp. 115–133.
- Sbeinati, M.R., Darawcheh, R., Mouty, M., 2005. The historical earthquakes of Syria: an analysis of large and moderate earthquakes from 1365 B.C. to 1900 A.D. *Annals in Geophysics* 48 (3), 347–435.
- Sharkov, E.V., 2000. Mesozoic and Cenozoic volcanism. In: Leonov, Yu.G. (Ed.), *Outline of Geology of Syria*. Nauka Press, Moscow, pp. 177–200 (in Russian).
- Sharkov, E.V., Chernyshev, I.V., Devyatkin, E.V., Dodonov, A.E., Ivanenko, V.V., Karpenko, M.I., Lebedev, V.A., Novikov, V.M., Hanna, S., Khatib, K., 1998. New data on the geochronology of Upper Cenozoic plateau basalts from north-eastern periphery of the Red Sea rift area (Northern Syria). *Doklady of Russian Academy of Sciences, Earth Section* 358 (1), 19–22.
- Simakova, A.N., 1993. Palynology and Pliocene – Quaternary climate history of the North-Western Syria. *Stratigraphy and Geological Correlation* 1 (3), 125–131.
- Simakova, A., Aleksandrova, G., Golovina, L., 2012. New Paleofloristic Data from Marine Late Pliocene–Pleistocene Deposits of Western Syria. In: *INQUA SEQS 2012 Meeting "At the Edge of the Sea: Sediments, Geomorphology, Tectonics, and Stratigraphy in Quaternary Studies"*. September 26–30, 2012, p. 90. Sassari, Sardinia, (Italy).
- Tchernov, E., 1999. The earliest hominids in the southern Levant. In: *Proceedings of the Intern. Conf. of Human Palaeontology, Orce, Spain, 1995*. Museo de Prehistoria y Paleontología, Orce, pp. 389–406.
- Trifonov, V.G. (Ed.), 2012. *Neotectonics, Recent Geodynamics and Seismic Hazard of Syria*. GEOS Publ., Moscow, 204 p.
- Trifonov, V.G., Bachmanov, D.M., Ali, O., Dodonov, A.E., Ivanova, T.P., Syas'ko, A.A., Kachaev, A.V., Grib, N.N., Imaev, V.S., Ali, M., Al-Kafri, A.M., 2012. Cenozoic tectonics and evolution of the Euphrates valley in Syria. In: Robertson, A.H.F., Parlak, O., Ünlügeng, U.C. (Eds.), *Geological Development of Anatolia and the Eastmost Mediterranean Region*, Geological Society, London, Special Publications, vol. 372. <http://dx.doi.org/10.1144/SP372.4>.
- Trifonov, V.G., Dodonov, A.E., Sharkov, E.V., Golovin, D.I., Chernyshev, I.V., Lebedev, V.A., Ivanova, T.P., Bachmanov, D.M., Rukieh, M., Ammar, O., Minini, H., Al Kafri, A.-M., Ali, O., 2011. New data on the Late Cenozoic basaltic volcanism in Syria, applied to its origin. *Journal of Volcanology and Geothermal Research* 199, 177–192.
- Trifonov, V.G., Karakhanian, A.S., 2004. *Geodynamics and the History of Civilization*. Nauka Press, Moscow, 668 p (in Russian with extended English summary).
- Trifonov, V.G., Trubikhin, V.M., Adjarian, J., Jallad, Z., El Hair, Yu., Ayed, H., 1991. Levant fault zone in the north-western Syria. *Geotectonics* 25 (2), 145–154.
- Westaway, R., 2004. Kinematic consistency between the Dead Sea Fault Zone and the Neogene and Quaternary left-lateral faulting in SE Turkey. *Tectonophysics* 391 (1–4), 203–237.
- Westaway, R., Demir, T., Seyrek, A., Beck, A., 2006. Kinematics of active left-lateral faulting in southeast Turkey from offset Pleistocene river gorges; Improved constraint on the rate and history of relative motion between the Turkish and Arabian plates. *Journal of the Geological Society of London* 163, 149–164.